

Accepted Manuscript

Marliolide inhibits skin carcinogenesis by activating NRF2/ARE to induce heme Oxygenase-1

June Lee, Karabasappa Mailar, Ok-Kyung Yoo, Won Jun Choi, Young-Sam Keum



PII: S0223-5234(18)30205-8

DOI: [10.1016/j.ejmech.2018.02.068](https://doi.org/10.1016/j.ejmech.2018.02.068)

Reference: EJMECH 10245

To appear in: *European Journal of Medicinal Chemistry*

Received Date: 25 August 2017

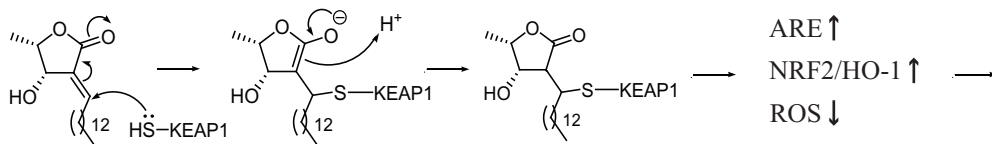
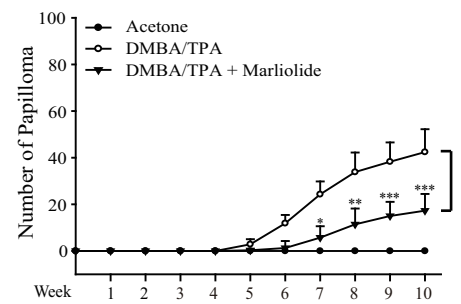
Revised Date: 14 February 2018

Accepted Date: 21 February 2018

Please cite this article as: J. Lee, K. Mailar, O.-K. Yoo, W.J. Choi, Y.-S. Keum, Marliolide inhibits skin carcinogenesis by activating NRF2/ARE to induce heme Oxygenase-1, *European Journal of Medicinal Chemistry* (2018), doi: 10.1016/j.ejmech.2018.02.068.

This is a PDF file of an unedited manuscript that has been accepted for publication. As a service to our customers we are providing this early version of the manuscript. The manuscript will undergo copyediting, typesetting, and review of the resulting proof before it is published in its final form. Please note that during the production process errors may be discovered which could affect the content, and all legal disclaimers that apply to the journal pertain.

ACCEPTED MANUSCRIPT

ARE \uparrow NRF2/HO-1 \uparrow ROS \downarrow 

Marliolide Inhibits Skin Carcinogenesis by Activating NRF2/ARE to Induce Heme Oxygenase-1

June Lee, Karabasappa Mailar, Ok-Kyung Yoo, Won Jun Choi* and Young-Sam Keum*

College of Pharmacy and Integrated Research Institute for Drug Development, Dongguk University, 32 Dongguk-ro, Goyang, Gyeonggi-do 10326, Korea

Corresponding authors

Won Jun Choi, Ph.D.

Phone: +82-31-961-5219. Fax: +82-31-961-5206. Email: mp89@dongguk.edu

Young-Sam Keum, Ph.D.

Phone: +82-31-961-5215. Fax: +82-31-961-5206. Email: keum03@dongguk.edu

ABSTRACT

Heme oxygenase-1 (HO-1) catalyzes the enzymatic degradation of heme to produce three anti-oxidant molecules: carbon monoxide (CO), ferrous ion (Fe^{2+}), and biliverdin. Induction of HO-1 is currently considered as a feasible strategy to treat oxidative stress-related diseases. In the present study, we identified marliolide as a novel inducer of HO-1 in human normal keratinocyte HaCaT cells. Mechanism-based studies demonstrated that the induction of HO-1 by marliolide occurred through activation of NRF2/ARE via direct binding of marliolide to KEAP1. Structure-activity relationship revealed chemical moieties of marliolide critical for induction of HO-1, which renders a support for Michael reaction as a potential mechanism of action. Finally, we observed that marliolide significantly inhibited the papilloma formation in DMBA/TPA-induced mouse skin carcinogenesis model and this event was closely associated with lowering the formation of 8-OH-G and 4-HNE *in vivo*. Together, our study provides the first evidence that marliolide might be effective against oxidative stress-related skin disorders.

1. Introduction

Oxidative stress is closely associated with aberrant exposure of reactive oxygen species (ROS, also known as oxygenated free radical molecules) such as superoxide (O_2^-), hydrogen peroxide (H_2O_2), and hydroxyl radical ($\cdot OH$) [1]. Although an adequate amount of ROS is necessary for maintaining proper redox homeostasis, a high amount of ROS is detrimental because it provokes direct oxidative damages on cellular macromolecules [2]. In order to deal with excessive oxidative stress, aerobic organisms possess a number of phase II cytoprotective enzymes including heme oxygenase-1 (HO-1), whose transcription is controlled by NF-E2-related factor 2 (NRF2) [3]. Under basal condition, NRF2 is constantly poly-ubiquitinated by Cullin-3 (Cul3)/Kelch-like ECH-associated protein 1 (KEAP1) in the cytoplasm. Upon exposure to pro-oxidants or electrophiles, NRF2 is released from Cul3/KEAP1, translocates into the nucleus, and activates HO-1 transcription by binding to the *cis*-acting element of promoter, termed antioxidant response element (ARE).

HO-1 is the first and rate-limiting enzyme in the heme degradation pathway to generate three anti-oxidant products: carbon monoxide (CO), ferrous ion (Fe^{2+}), and biliverdin [4]. CO protects lungs and hearts against endotoxin, ischemia/reperfusion injury, cardiac xenograft rejection, and asthma by modulating cytokine production, cell proliferation, and apoptosis [5]. Biliverdin and its reduced product bilirubin are efficient scavengers of ROS [6]. Ferrous iron induces ferritin expression and contributes to iron sequestration [7]. Collectively, these imply that all enzymatic products of HO-1 possess beneficial activities. Supporting this idea, HO-1 knock-out mice spontaneously develop inflammatory diseases and are highly susceptible to experimental sepsis [8]. Phenotypical alterations of individuals with genetic HO-1 deficiency are also similar to those observed in HO-1 knock-out mice [9].

Marliolide (Fig. 1A) is a natural product having γ -lactone ring with α,β -unsaturated carbonyl group, which was firstly isolated from the leaves of *Mollinedia marliae* and the bark of *Cinnamomum cambodianum* [10, 11]. However, there exist no literatures demonstrating the pharmacological activity and related biochemical mechanisms of marliolide. In the present study, we demonstrate that marliolide strongly induced HO-1 in human normal keratinocyte HaCaT cells. We also demonstrate that marliolide could form a stable adduct with KEAP1 and activate NRF2/ARE to induce HO-1. Finally, we provide evidence that marliolide protects mice against oxidative damages *in vivo*, thereby exhibiting significant skin chemopreventive activity.

ACCEPTED MANUSCRIPT

2. Results

2.1. Marliolide Induce HO-1 by NRF2-dependent ARE activation

Induction of phase II cytoprotective enzymes, including HO-1 has been recognized as a feasible strategy to suppress carcinogenesis and other chronic diseases caused by oxidants and electrophiles [12]. In addition, recent studies demonstrate that HO-1 can suppress immune-mediated inflammatory disorders by limiting innate or adaptive immune responses [13] or by promoting polarization of macrophages towards an anti-inflammatory M2 phenotype [14]. Therefore, it is not surprising to observe that numerous HO-1 chemical inducers were effective for treatment of chronic inflammatory disorders [15]. In accordance with this, we have attempted to find new HO-1 inducers and found that marliolide strongly induced HO-1 (Fig. 1B) without perturbing cellular integrity in human keratinocyte HaCaT cells: marliolide did not affect the cell-cycle pattern (Fig. 1C) and the viability (Fig. 1D), and failed to induce apoptosis (Fig. 1E).

To examine whether marliolide could activate ARE-dependent gene expression, we subcloned DNA oligonucleotides containing 3x ARE sequence into pGreenFire dual reporter plasmid and established stable HaCaT-ARE-GFP-luciferase cells by lentiviral transduction and subsequent selection with puromycin (Fig. 2A). To examine whether HaCaT-ARE-GFP-luciferase cells are responsive to ARE inducer, we exposed sulforaphane, a prototypical inducer of ARE, to HaCaT-ARE-GFP luciferase cells and found that it significantly increased ARE luciferase activity in HaCaT-ARE-GFP-luciferase cells (Fig. 2B). Likewise, marliolide increased ARE-dependent GFP expression (Fig. 2C) and the luciferase activity of HaCaT-ARE-GFP-luciferase cells in dose- (Fig. 2D, Left Panel) and time-dependent manner (Fig. 2D, Right Panel).

Because NRF2 is a leucine-zipper transcription factor responsible for ARE-dependent gene activation [16], we exposed marliolide to HaCaT cells and measured NRF2 level. Our results showed that marliolide increased NRF2 level in dose- (Fig. 3A, Upper Panel) and time-dependent manner (Fig. 3A, Lower Panel). Marliolide also caused translocation of NRF2 into the nucleus (Fig. 3B). To examine whether the induction of HO-1 by marliolide was dependent on Nrf2 genotype, we have prepared Nrf2 (+/+) and Nrf2 (-/-) mouse embryonic fibroblasts (MEFs) (Fig. 3C, Upper Panel) and exposed them to marliolide. As a result, the induction of HO-1 by marliolide was attenuated in Nrf2 (-/-) MEFs, compared to that in Nrf2 (+/+) MEFs (Fig. 3C, Lower Panel). The induction of HO-1 mRNA level by

marliolide was also significantly attenuated in Nrf2 (-/-) MEFs compared that in Nrf2 (+/+) MEFs (Fig. 3D). These results illustrate that marliolide induction of HO-1 occurs through NRF2/ARE activation.

2.2. Chemistry

We have recently reported the asymmetric total synthesis of marliolide **2** [17]. Synthesis of marliolide **2** and its (*Z*)-isomer **3** is described in Fig. 4A. With marliolide **2** in hand, we prepared saturated marliolide **4** by catalytic hydrogenation of **2** using H₂, Pd/C (5%) in presence of acetic acid [18]. Interestingly, along with the hydrogenated product **4** (73%), we isolated and identified compound **5** (10%) in minor proportion, which is formed by the hydrogenation of alkene and coincident dehydroxylation at β -position (Fig. 4B). During our attempt to synthesize β -keto- γ -butyrolactone by oxidation of secondary hydroxyl group in marliolide, we obtained compound **6** from unexpected rearrangement. Hence, to check out the effects of β -hydroxyl group, we turned our attention to synthesizing compound **8** without affecting other functionalities of **2**. First, hydrogenation of internal olefinic bond in **6** using H₂, Pd/C (5%) in presence of acetic acid afforded compound **7**, followed by elimination of secondary alcohol produced the desired compound **8** (Fig. 4B). Further, compound **9** was prepared by reacting **2** with isovaleryl chloride in presence of DMAP. To investigate the effect of chirality of γ -methyl in marliolide, we utilized our strategy to synthesize *epi*-marliolide **11** by way of the known sequential reactions (Fig. 4C). Condensation of the key intermediate lactone *epi*-**1** with myristyl aldehyde, selective protection of resulting diastereomeric diol with TBS, and mesylation of remaining alcohol followed by elimination afforded **10** in 16% yield for three steps. Finally, treatment of **10** with HCl produced the desired epimer of marliolide, **11** [17]. A series of marliolide derivatives **22-31** with different chain length at α -position were also prepared according to the previously reported general methods (Fig. 4D).

2.3. Structure Activity Relationship of Marliolide

It is generally accepted that NRF2/ARE-dependent gene activation by chemicals largely occurs via three ways: (1) direct conjugation and subsequent inactivation of KEAP1 by Michael reaction [19], (2) direct inhibition between NRF2 and KEAP1 interface [20], and (3) activation of intracellular signaling pathways, leading to NRF2 transactivation [21]. A close examination of marliolide structure shows that it contains α,β -unsaturated lactone

moiety belonging to Michael acceptor class. This intrigued us to examine whether marliolide induction of HO-1 could be attributable to its binding to KEAP1. After synthesizing biotinylated marliolide (please refer to Supporting information), we incubated biotin and biotinylated marliolide (Fig. 5A, Left Panel) with HaCaT cell lysates and performed an immunoprecipitation with streptavidin-agarose bead followed by Western blotting with KEAP1 and NRF2 antibodies. As a result, we observed that biotinylated marliolide could selectively bind to KEAP1, but not NRF2 (Fig. 5A, Right Panel).

After setting up a hypothetical mechanism of HO-1 induction by marliolide: marliolide binds to KEAP1 through Michael reaction (Fig. 5B), we synthesized a number of marliolide derivatives and examined their effects on HO-1 level in HaCaT cells (Fig. 5C). As expected, marliolide (**2**) caused a strong time-dependent induction of HO-1. **3** also induced HO-1, although its induction kinetic was retarded compared with **2**. However, **4** failed to induce HO-1, providing a convincing clue that marliolide induction of HO-1 might occur via Michael reaction. This hypothesis could be further examined by the use of another marliolide derivative, in which the carbonyl group of the γ -butyrolactone ring was reduced into the hydroxyl group. In spite of repetitive efforts, however, we failed to synthesize this derivative due to its intrinsic instability: this might be due to hemi-ketal formation and subsequent opening of γ -butyrolactone ring (Data not shown). In addition, we observed that both **5** and **8** failed to induce HO-1. The failure of **5** to induce HO-1 was somewhat unexpected in that the hydroxyl group of γ -butyrolactone ring did not seem to participate in Michael reaction. Although the exact reason is unclear, the observation that **9** failed to induce HO-1 renders a strong support that hydroxyl group in γ -butyrolactone ring is critical for the induction of HO-1 by marliolide. Finally, we observed that **11** induced HO-1, although its induction kinetic was slower than **2**. This indicates that configuration of hydroxyl group does not significantly interfere with the ability of marliolide to induce HO-1.

We conducted a second set of SAR study to ask whether varying the aliphatic chain length of marliolide could affect the degree of HO-1 induction (Fig. 5D). We observed that both **22** and **23** failed to induce HO-1. When compared with **2**, **24** exerted a weaker and **25** exhibited a retarded induction of HO-1. In contrast, **26**, **27**, **28**, and **29** seemed to exhibit equivalent induction of HO-1 compared with **2**, while **30** and **31** exerted a weaker or delayed induction of HO-1 compared with **2**. To quantitatively compare the induction level of HO-1 mRNA, we exposed **2**, **26**, **27**, **28**, and **29** to HaCaT cells and conducted real-time RT-PCR

assay at different time points with HO-1 specific primers. Compared with **2**, **29** exhibited a stronger induction of HO-1 mRNA at 4 h post-treatment, **26**, **27**, **28**, and **29** exhibited a stronger induction of HO-1 mRNA at 8 h post-treatment, and **26** and **27** exhibited a stronger induction of HO-1 mRNA at 12 h post-treatment (Fig. 5D). This result suggests that **26**, **27**, **28**, and **29** can exhibit a stronger induction of HO-1 mRNA than marliolide *in vitro*, depending on the exposure time. Finally, our MTT assay result showed that all marliolide derivatives used in the present study were not cytotoxic to HaCaT cells (Fig. 5E).

2.4. Marliolide Attenuates DMBA/TPA-induced Papilloma Formation in Hairless Mice.

Because marliolide strongly induced NRF2/ARE-dependent HO-1 in HaCaT cells, we examined whether marliolide could induce NRF2 and phase II cytoprotective enzymes *in vivo*. To address this issue, we have topically applied marliolide and **29**, which induced HO-1 mRNA comparably or stronger than marliolide (Fig. 5D) in the back of hairless mice and conducted Western blotting using mouse skin lysates. Our results showed that both marliolide and **29** increased the expression of NRF2 and phase II cytoprotective enzymes (HO-1 and GCLC) in mouse skin (Fig. 6A). Because carcinogenesis requires multiple genetic mutations that can be facilitated by exposure to oxidative stress [22], we assumed that marliolide would exhibit anti-oxidant activities through induction of NRF2/HO-1 to inhibit carcinogenesis *in vivo*. We adopted DMBA/TPA two-stage mouse skin carcinogenesis model to address this question. During the course of study, topical application of marliolide significantly suppressed the number (Fig. 6B, Upper Panel) and incidence (Fig. 6B, Lower Panel) of DMBA/TPA-induced papilloma in the back of hairless mice. At autopsy, we observed that marliolide inhibited the growth of DMBA/TPA-induced papilloma (Fig. 6C) and suppressed the *in vivo* formation of 8-hydroxyguanosine (8-OH-G) and 4-hydroxynoneal (4-HNE) (Fig. 6D), both of which are well-known oxidative stress markers. These results suggest that marliolide exhibits significant anti-oxidant and anti-carcinogenic effects *in vivo*.

3. Conclusion

Previous studies have demonstrated that induction of NRF2/HO-1 can alleviate diverse oxidative stress-related disorders such as cancer [23], diabetes [24], cardiovascular diseases [25, 26]. In addition, natural compounds that possess the ability to induce HO-1 and NRF2 can inhibit development of inflammatory diseases [27, 28]. Therefore, exploring new NRF2/HO-1 activators for treatment of pro-inflammatory diseases aroused significant commercial interests in the last decade. One example is an oral formulation of dimethyl fumarate (DMF), which was developed for patients with recurrent multiple sclerosis (MS) and finally approved by the Food and Drug Administration in 2013 [29]. In line with this idea, we found that marliolide was not cytotoxic (Fig. 1) and strongly induced HO-1 by eliciting NRF2-dependent ARE activation in HaCaT cells (Fig. 2 and 3). Our results also showed that marliolide induced HO-1 by acting as Michael acceptor for KEAP1, but not NRF2 (Fig. 5A). In addition, SAR study revealed chemical moieties of marliolide responsible for the induction of HO-1 (Fig. 5C). It is known that KEAP1 contains 25 cysteine residues in mouse and 27 cysteine residues in human [30]. In particular, some cysteine residues of KEAP1 are located adjacent to basic amino acid residues. Therefore, KEAP1 seems to contain reactive cysteine residues with low pK_a values, which might serve as excellent targets for Michael reaction. However, evidence is still lacking on which cysteine residue(s) of KEAP1 form a direct adduct with marliolide, although several cysteine residues of KEAP1 (Cys 151, Cys 273 and Cys 288, for example) were previously proposed as preferential sites for Michael reaction [31].

Our results show that marliolide and **29** are efficient inducers of NRF2 and its downstream targets *in vivo* (Fig. 6A). Using DMBA/TPA two-stage mouse skin carcinogenesis model, we observed that marliolide significantly inhibited the incidence of papilloma in hairless mice (Fig. 6B). The inhibition of papilloma formation by marliolide could be ascribed to its ability to induce NRF2-dependent phase II cytoprotective enzymes (Fig. 6A) and lower the degree of oxidative stress *in vivo* (Fig. 6D). Moreover, we note that **26**, **27**, **28**, and **29** elicited a stronger induction of HO-1 mRNA than marliolide (Fig. 5D) at certain time points without apparent cytotoxicity in HaCaT cells (Fig. 5E). This raises a possibility that **26**, **27**, **28**, and **29** could be further harnessed as novel pharmacological leads of NRF2/HO-1 inducers. Because **26** [(-)-licunolide B] [32], **28** [(-)-lincomolide B] [33] and **30** [(-)-isodihydromahubanolide B] [34] were found in particular species of fungus or plants,

it is possible to speculate that **27** and **29** might exist somewhere in nature. However, the exact roles of these marliolide derivatives are currently unclear.

ACCEPTED MANUSCRIPT

4. Experimental Section

4.1. Cell Culture, Chemicals, Plasmids, and Antibodies

DMEM, RPMI, FBS, and penicillin/streptomycin (Pen/Strep) were purchased from WELGENE (Daegu, Korea). HaCaT cells were purchased from Korean Cell line Bank (Seoul, Korea). HaCaT cells were grown in RPMI media supplemented with 10% FBS and Penicillin/Streptomycin (100 U/ml). Sulforaphane, DMBA, TPA, etoposide, and antibodies against NRF2, KEAP1, total actin, 8-OH-G were purchased from Santa Cruz biotechnology (Santa Cruz, CA, USA). Polybrene was purchased from Merck-Millipore (Merck-Millipore Korea, Daejeon, Korea). pGreenfire reporter vector was purchased from System Bioscience (Palo Alto, CA, USA). Lentiviral helper plasmids (pMD2.G and psPAX.2) were acquired from Addgene (Cambridge, MA, USA). 3x Tandem ARE DNA oligonucleotides were bought from Macrogen (Seoul, Korea), annealed, and subcloned into pGreenfire vector using a double-digestion with Cla1 and Spe1 restriction enzymes. HO-1 antibody was purchased from Enzo Life Science (Farmingdale, NY, USA). Antibodies against GCLC, Cleaved-Caspase-3 and Cleaved-PARP were purchased from Cell Signaling Technology (Beverly, MA, USA). 4-HNE antibody was purchased from Abcam (Cambridge, MA, USA). Marliolide and all derivatives were dissolved in DMSO (vehicle) and used in all *in vitro* experiments at a dilution ratio of 1/1000.

4.2. Measurement of Cell-Cycle by Fluorescence-activated Cell Sorting (FACS).

After treatment of marliolide, an equal number of HaCaT cells (1×10^6 /group) was dispensed into glass tubes and fixed with a solution containing 1x PBS and 70% EtOH at a ratio of 3:7. After washing with 1x PBS, cells were mixed with propidium iodide (20 μ g/ml) and the changes in cell-cycle were measured by FACS Calibur flow cytometer (Becton Dickinson, San Jose, CA, USA).

4.3. Immunofluorescence (IF) Assay

After treatment of marliolide, confluent HaCaT cells were grown on a slice glass and incubated with blocking serum (1% BSA) for 30 min. After washing with 1x PBS, HaCaT cells were fixed with paraformaldehyde and hybridized with primary antibodies overnight at 4°C. These slides were washed with 1x PBS and probed with fluorescein isothiocyanate (FITC)-conjugated rabbit secondary antibodies (Jackson-ImmunoResearch, West Grove, PA,

USA). The fluorescent images were obtained with C2 confocal microscope (Nikon Korea, Seoul, Korea).

4.4. Generation of HaCaT-GFP-luciferase Cells by Lentiviral Transduction

Using JETPEI reagent (Polyplus-Transfection, New York, NY, USA), 293T packaging cells were transfected with 3 μ g pGreenFire-ARE plasmid together with lentiviral helper vectors (3 μ g pMD2.G and 3 μ g psPAX.2). After 48 h transfection, viral supernatant was collected, filtered, and transduced into confluent HaCaT cells, which were further selected with puromycin (1 μ g/ml) for 48 h.

4.5. Monitoring GFP and Luciferase Activity in HaCaT-ARE-GFP-luciferase Cells

Established HaCaT-ARE-GFP-luciferase cells were plated in 24-well culture plates at a density of 2×10^5 cells/well. After treatment of marliolide, cellular GFP expression was observed by fluorescent microscopy. For the luciferase assay, HaCaT-ARE-GFP-luciferase cells were washed with 1x PBS and lysed with luciferase lysis buffer [0.1 M potassium phosphate buffer at pH 7.8, 1 % Triton X-100, 1 mM DTT, 2 mM EDTA]. The luciferase activities were measured by GLOMAX Multi-system. (Promega, Madison, WI, USA) and normalized by protein concentration.

4.6. Western Blot Analysis

After treatment of marliolide and derivatives, cultured cells were collected and washed with ice-cold 1x PBS buffer. Cells were collected by centrifugation and resuspended with RIPA lysis buffer [50 mM Tris-HCl at pH 8.0, 150 mM NaCl, 1% NP-40, 0.5% deoxycholic acid, 0.1% sodium dodecyl sulfate (SDS), 1 mM Na_3VO_4 , 1 mM dithiothreitol (DTT), 1 mM phenylmethylsulfonyl fluoride (PMSF)] on ice for 30 min. Cell lysates were collected and protein concentration was measured by BCA Protein Assay Kits (Thermo-Fisher Scientific, Waltham, MA, USA). Equal amounts of cell lysates were resolved by SDS-PAGE and transferred to PVDF membranes. After 1 h incubation in blocking buffer (5% skin milk in 1x PBST), the membrane was hybridized with appropriated primary antibodies overnight at 4 °C. After washing with 1x PBST three times, the membranes were hybridized with HRP-conjugated secondary antibodies (Thermo Fischer scientific, Waltham, MA, USA). After washing with 1x PBST three times, the membranes were finally visualized by ECL detection system. Total actin blot was used as a control to illustrate an equal loading of

samples.

4.7. Real-time Reverse Transcription-Polymerase Chain Reaction (RT-PCR)

After treatment of marliolide and derivatives, HaCaT cells were collected and total RNA was extracted by Hybrid-R RNA extraction kit (GeneAll, Seoul, Korea). Total RNA was subject to cDNA synthesis using PrimeScript RT-PCR kit (TAKARA Korea, Seoul, Korea). Real-time RT-PCR analysis was performed using SYBR mix on CFX384 Real-time system (BioRad, Hercules, CA, USA). Amplification protocol comprises following PCR cycles: a single cycle of 5 min at 95 °C, 40 cycles of 10 sec at 95 °C, 10 sec at 59 °C, and 20 sec 72 °C, and a final cycle of 10 sec at 95 °C. Real-time PCR primers used in the present study are as follows: HO-1 PCR primers [5'-ATGCCCCAGGATTTGTCAGA-3' (Forward) and 5'-ACCTGGCCCTTCTGAAAGTT-3' (Reverse)] and GAPDH PCR primers [5'-CAC AGTCCATGCCATCACTG-3' (Forward) and 5'-GTCCACCACTGACACGTTG-3' (Reverse)]. The relative mRNA level of HO-1 was normalized by that of GAPDH.

4.8. MTT assay.

HaCaT cells were seeded in 96 well plate (30,000 cells/well) and exposed to marliolide or its derivatives for 24 h. After washing with 1x PBS, cells were incubated with 100 µl MTT solution (5 mg/ml) for 4 h. After a lysis with 100 µl DMSO, the resulting absorbance was measured by spectrophotometer at the wavelength of 560 nm.

4.9. Immunoprecipitation of KEAP1 by Biotinylated Marliolide

Confluent HaCaT cells were lysed with RIPA buffer. HaCaT lysates (800 µg) were then mixed with biotin (10 nmole) and biotinylated marliolide (10 nmole) followed by immunoprecipitation with streptavidin-agarose bead (Cell Signaling Technology, Waltham, MA, USA) overnight at 4 °C. After washing beads with ice-cold 1x PBS buffer, Western blot analysis was conducted using KEAP1 and NRF2 antibodies.

4.10. DMBA/TPA-induced Two-Stage Mouse Skin Carcinogenesis Model

Six-week male hairless mice were purchased from Daehan Biolink (Eumseong, Korea). Animals were housed in sterile filter-capped microisolator cages and provided with water and diet *ad libitum*. After a week acclimation, individual mice were topically applied with acetone (vehicle) or DMBA (2 µmole) once in the first week. Starting from the second

week, the back of hairless mice were applied with TPA (10 nmole) alone or in combination with marliolide (10 μ mole) three times per week. During the course of experiment, the number of papilloma was manually counted at the end of every week. At sacrifice, mouse skin was immersed 30% formalin and embedded in paraffin block. After preparation of slides, hematoxylin/eosin (H/E) staining was conducted and the images were captured by phase-contrast microscopy. For immunofluorescence (IF) assay, the slides were hybridized with primary 8-OH-G and 4-HNE antibodies overnight at 4 °C and probed with FITC-conjugated secondary antibodies (Jackson ImmunoResearch, West grove, PA, USA). The fluorescent image were obtained with C2 confocal microscope (Nikon Korea, Seoul, Korea). The animal experiment was carried out under an Institutional Animal Care and Use Committee-approved Protocol (IACUC-2015-066) from Dongguk University (Seoul, Korea).

4.11. Statistics

Statistical analysis was conducted using Student's t-test. Asterisks indicate a statistical significance with *P<0.05, **P<0.01 and *** p<0.001.

4.12. General Chemical Procedures

Except where noted, all the materials were purchased from commercial suppliers and used without further purification. All reactions were routinely carried out under an inert atmosphere of dried nitrogen, in hot-oven dried glassware. Proton nuclear magnetic resonance (¹H-NMR) Spectra (CDCl₃, DMSO-*d*₆) were recorded on a Varian (400 MHz) spectrometer (Varian Medical Systems, Inc., Palo Alto, CA, USA). The 1H-NMR data are reported as peak multiplicities: s for singlet, d for doublet, dd for doublet of doublets, t for triplet, q for quartet, br s for broad singlet and m for multiplet. ¹³C-NMR spectra (CDCl₃, DMSO-*d*₆) were recorded on Varian (100 MHz) spectrometer. The chemical shifts are reported as parts per million (ppm), downfield from tetramethylsilane (TMS) internal standard relative to the solvent peak with coupling constants in hertz (Hz). Optical rotations were determined on Jasco P-2000 polarimeter in appropriate solvent. Infrared spectra were recorded on FT-IR (NICOLET-iS5). Melting points were measured on Thermoscientific-9200. Elemental analyses (C, H) were used to determine purity of all synthesized compounds, and the results were within \pm 0.4% of the calculated values, confirming > 95% purity (EA1110 CHNS-0, CE Instrument, Italy). Reactions were monitored with TLC (Merck precoated 60F254 plates). Spots were detected by viewing under a UV light, colorizing with charring

after dipping in anisaldehyde solution or basic KMnO_4 solution. Column chromatography was performed on silica gel 60 (230-400 mesh Kieselgel 60). The mass spectra were recorded using LRMS (electron ionization MS) obtained on a Shimadzu-2020 or using HRMS (electrospray ionization MS) obtained on a G2 QTOF mass spectrometer.

4.13. Synthetic Procedures of Marliolide and Its Derivatives

(E,4S,5S)-Dihydro-4-hydroxy-5-methyl-3-tetradecylidenefuran-2(3H)-one, marliolide (2). Marliolide **2** was obtained as off-white solid in accordance with reported procedure [17] starting from D-ribose: mp 72-74 °C; $[\alpha]_{\text{D}}^{20} = -92.0$ (c=1.0, CHCl_3); ^1H NMR (400 MHz, CDCl_3) δ 6.97-6.93 (t, $J = 8.0$ Hz, 1H), 4.83-4.81 (t, $J = 5.2$ Hz, 1H), 4.56-4.50 (m, 1H), 2.45-2.34 (m, 2H), 1.65-1.59 (m, 1H), 1.56-1.50 (m, 2H), 1.45 (d, $J = 6.8$ Hz, 3H), 1.39-1.25 (bs, 20H), 0.88 (t, $J = 6.4$ Hz, 3H); ^{13}C NMR (100 MHz, CDCl_3) δ 169.9, 147.8, 130.5, 78.7, 67.8, 31.9, 29.9-29.4, 28.4, 22.7, 14.1, 14.0; IR (neat) 3383, 2920, 2846, 1745, 1692, 1212, 1050 cm^{-1} ; HRMS (ESI) m/z calcd for $\text{C}_{19}\text{H}_{34}\text{O}_3$ $[\text{M}+\text{H}]^+$: 311.2583, found: 311.2583; Anal. calculated for $\text{C}_{19}\text{H}_{34}\text{O}_3$: C, 73.50; H, 11.04, found: C, 73.48; H, 11.03.

(Z,4S,5S)-Dihydro-4-hydroxy-5-methyl-3-tetradecylidenefuran-2(3H)-one (3). Compound **3** was obtained as off-white solid in accordance with reported procedure [17]: mp 55-57 °C; $[\alpha]_{\text{D}}^{20} = -50.1$ (c=0.6, CHCl_3); ^1H NMR (400 MHz, CDCl_3) δ 6.58-6.54 (t, $J = 6.4$ Hz, 1H), 4.66-4.64 (t, $J = 5.6$ Hz, 1H), 4.56-4.52 (m, 1H), 2.80-2.68 (m, 2H), 1.70 (d, $J = 6.0$ Hz, 1H), 1.50-1.42 (m, 2H), 1.39 (d, $J = 6.4$ Hz, 3H), 1.39-1.25 (bs, 20H), 0.88 (t, $J = 6.4$ Hz, 3H); ^{13}C NMR (100 MHz, CDCl_3) δ 168.9, 149.9, 129.2, 77.9, 71.4, 31.9, 29.7-29.4, 29.3, 28.8, 27.9, 22.6, 14.1, 14.1; IR (neat) 3383, 2920, 2846, 1745, 1692, 1212, 1050 cm^{-1} ; LCMS (ESI) m/z calcd for $\text{C}_{19}\text{H}_{34}\text{O}_3$ $[\text{M}+\text{H}]^+$: 311.26, found: 311.35; Anal. calculated for $\text{C}_{19}\text{H}_{34}\text{O}_3$: C, 73.50; H, 11.04, found: C, 73.35; H, 10.01.

(3R,4S,5R)-3-Dihydro-4,5-dihydroxy-3-tetradecylfuran-2(3H)-one (4) and (3R,5R)-3-Dihydro-5-hydroxy-3-tetradecylfuran-2(3H)-one (5). To a stirred solution of **2** (30 mg, 0.096 mmol) in ethanol (1 ml), were added 5% Pd/C (5 mg) and AcOH, and the suspension was stirred overnight under an atmosphere of hydrogen at room temperature. The resulting suspension was filtered through a pad of celite and the filtrate was evaporated. The crude residue was purified by silica gel column chromatography (hexanes/EtOAc=9:1 v/v) to afford **4** (22 mg, 73%) as off-white solid: mp 91-93 °C; $[\alpha]_{\text{D}}^{20} = -33.3$ (c=1.0, CHCl_3); ^1H NMR (400

MHz, CDCl₃) δ 4.48-4.42 (m, 1H), 4.31 (t, J = 3.8 Hz, 1H), 2.54 (m, 1H), 2.32 (bs, 1H), 1.85-1.76 (m, 1H), 1.7-1.58 (m, 1H), 1.44 (d, J = 6.4 Hz, 3H), 1.44-1.39 (bm, 2H), 1.3-1.25 (bs, 22H), 0.88 (t, J = 6.6 Hz, 3H); ¹³C NMR (100 MHz, CDCl₃) δ 178.1, 79.1, 71.1, 47.6, 29.3-29.7, 31.9, 27.6, 23.3, 22.7, 14.1, 13.7; IR (neat) 2913, 2851, 1731, 1588, 1203 cm⁻¹; HRMS (ESI) m/z calcd for C₁₉H₃₆O₃ [M+H]⁺: 313.2743, found: 313.2758; Anal. calculated for C₁₉H₃₆O₃: C, 73.03; H, 11.61, found: C, 73.38; H, 11.73. Unintended minor product, compound **5** (3 mg, 10.4%) was obtained as off-white solid: mp 58-60 °C; $[\alpha]_{\text{D}}^{20}$ = -11.9 (c=0.28, CHCl₃); ¹H NMR (400 MHz, CDCl₃) δ 4.46 (m, 1H), 2.63-2.55 (m, 1H), 2.5-2.43 (m, 1H), 1.95-1.89 (bm, 1H), 1.46 (m, 1H), 1.42 (d, J = 6.0 Hz, 3H), 1.31-1.25 (bs, 25H), 0.88 (t, J = 6.6 Hz, 3H); ¹³C NMR (100 MHz, CDCl₃) δ 179.0, 75.0, 41.5, 37, 31.9, 30.3, 29.3-29.6, 27.4, 22.6, 21.0, 14.1; IR (neat) 2918, 2846, 1757, 1466, 1206 cm⁻¹; HRMS (ESI) m/z calcd for C₁₉H₃₆O₂ [M+H]⁺: 297.2794, found: 297.2637; Anal. calculated for C₁₉H₃₆O₂: C, 76.97; H, 12.24, found: C, 76.89; H, 12.23.

(S)- 3-(1-Hydroxytetradecyl)-5-methylfuran-2(5H)-one (6). To a solution of **2** (15 mg, 0.05 mmol) in acetone (1 ml), Jones reagent (0.5 ml (prepared from 35 mg of Cr₂O₃ + 0.03 ml of conc. H₂SO₄ + 0.5 ml of water at 0 °C)) was added at 0 °C. Reaction mixture was slowly warmed to room temperature and stirred for 3 h. The reaction mixture was quenched with sat. NaHCO₃ solution and extracted with ethyl acetate. Combined organic layer was dried over MgSO₄, filtered and evaporated. The crude residue was purified by silica gel column chromatography (hexanes/EtOAc=9:1 v/v) to give **6** (10 mg, 66%) as off-white solid: ¹H NMR (400 MHz CDCl₃) δ 7.19 (m, 1H), 5.09-5.04 (m, 1H), 4.48 (m, 1H), 1.81-1.63 (m, 2H), 1.45 (d, J =6.8 Hz, 3H), 1.25 (bs, 21H), 0.88 (t, J =8.6 Hz, 3H).

(5S)-Dihydro-3-(1-hydroxytetradecyl)-5-methylfuran-2(3H)-one (7). To a stirred solution of **6** (10 mg, 0.03 mmol) in ethanol (1 ml), were added catalytic amount of AcOH and 5% Pd/C (2 mg) and the flask was sealed with a hydrogen balloon. The suspension was stirred at room temperature for 1 h. The resulting suspension was filtered through a pad of celite and the filtrate was evaporated. The crude residue was purified by silica gel column chromatography (hexanes/EtOAc=9:1 v/v) to afford **7** (10 mg, 99%) as off-white solid: ¹H NMR (400 MHz, CDCl₃) δ 4.49-4.41 (m, 1H), 4.19 (m, 1H), 2.78 (m, 1H), 2.61 (m, 1H), 2.43 (m, 1H), 2.04-1.95 (bm, 2H), 1.45 (m, 8H), 1.25 (bs, 42H), 0.89 (m, 6H).

(*E,S*)-Dihydro-5-methyl-3-tetradecylidenefuran-2(3*H*)-one (8). To a solution of **7** (10 mg, 0.03 mmol) in methylene chloride (1.0 ml), triethylamine (0.06 ml, 0.48 mmol) and methanesulfonyl chloride (0.01 ml, 0.16 mmol) were added at 0 °C and the reaction mixture was stirred at the same temperature for 3 h. Excess TEA (0.06 ml, 0.48 mmol) was added and the reaction mixture was slowly warmed to 45 °C and maintained overnight. Reaction completion was monitored by TLC. Reaction mixture was diluted with methylene chloride and washed with sat. NaHCO₃ solution. Organic layer was dried over MgSO₄, filtered and evaporated. The crude residue was purified by silica gel column chromatography (hexanes/EtOAc=9.8:0.2 v/v) to afford **8** (1.6 mg, 17%, ***E*-isomer**) as white solid: ¹H NMR (400 MHz, CDCl₃) δ 6.7-6.75 (m, 1H), 4.69-4.64 (m, 1H), 3.02 (m, 1H), 2.43-2.37 (m, 1H), 2.18-2.12 (m, 2H), 1.48 (m, 2H), 1.42 (d, *J* = 6.4 Hz, 3H), 1.25 (bs, 20H), 0.89 (t, *J* = 6.8 Hz, 3H).

(*E,2S,3S*)-Tetrahydro-2-methyl-5-oxo-4-tetradecylidenefuran-3-yl 3-methylbutanoate (9). To a stirred solution of **2** (25 mg, 0.08 mmol) in methylene chloride (2 ml), were added DMAP (49 mg, 0.41 mmol) and isovaleryl chloride (73 mg, 0.61 mmol). The reaction mixture was stirred at room temperature overnight. The reaction mixture was quenched with sat. NaHCO₃ solution and extracted in methylene chloride (3 times). Combined organic layer was washed with brine solution, dried over MgSO₄, filtered and evaporated. The crude residue was purified by silica gel column chromatography (hexanes/EtOAc=9:1 v/v) to afford **9** (25 mg, 79%) as a syrupy solid: [α]_D²⁰ = -73.5 (c=0.88, CHCl₃); ¹H NMR (400 MHz, CDCl₃) δ 6.98 (dt, *J* = 8.0, 1.4 Hz, 1H), 6.06 (d, *J* = 4.8 Hz, 1H), 4.69-4.63 (m, 1H), 2.29-2.22 (m, 2H), 2.25 (d, *J* = 7.2 Hz, 2H), 2.15-2.08 (m, 1H), 1.48 (m, 2H), 1.35 (d, *J* = 6.0 Hz, 3H), 1.25 (bs, 20 H), 0.97 (s, 3H), 0.96 (s, 3H), 0.88 (t, *J* = 6.8 Hz, 3H); ¹³C NMR (100 MHz, CDCl₃) δ 172.1, 169.2, 148.8, 126.7, 68.2, 43, 31.9, 30.2, 29.6-29.3, 28.2, 25.6, 22.6, 22.3, 14.2, 14.1; IR (neat) 2926, 2853, 1767, 1737, 1680, 1455, 1289, 1112, 989, 759 cm⁻¹; HRMS (ESI) *m/z* calcd for C₂₄H₄₂O₄ [M+H]⁺: 395.3161, found: 395.3169; Anal. calculated for C₂₄H₄₂O₄: C, 73.05; H, 10.73, found: C, 73.58; H, 10.63.

(*E,4R,5S*)-Dihydro-4--(*tert*-butyldimethylsilyl)-5-methyl-3-tetradecylidenefuran-2(3*H*)-one (10). To a stirred solution of lithium diisopropylamide (20.37 mmol, 2.0 M in heptane) in THF (2 ml) at -78 °C, was added a solution of ***epi*-1** (500 mg, 4.31 mmol) in THF (5 ml) dropwise via syringe under N₂ atmosphere. After 2 h of stirring, a solution of myristyl

aldehyde (1.1 g, 5.17 mmol) in dry THF (5 ml) and HMPA (5 ml) was added dropwise via syringe at $-78\text{ }^{\circ}\text{C}$ and the reaction mass was allowed to warm to $-30\text{ }^{\circ}\text{C}$ over a period of 3 h and the same temperature was maintained for 3 h. The reaction mixture was quenched with 30 ml of sat. NH_4Cl and extracted with EtOAc (50ml x 3). Combined organic layer washed with sat. brine, dried over MgSO_4 , filtered and evaporated. The crude residue was purified by silica gel column chromatography (EtOAc/ CH_2Cl_2 =0-20% EtOAc) gave diastereomeric mixture product diol (384 mg). The purified product was taken for next step without further analysis. To a stirred solution of above product (1.17 mmol) in DMF (4 ml) at RT, imidazole (2.34 mmol) and *tert*-butyldimethylchlorosilane (1.4 mmol) were added under N_2 atmosphere and the reaction mixture was stirred for overnight. Reaction mixture was quenched with sat. NaHCO_3 and extracted with EtOAc. Organic layer was dried over MgSO_4 , filtered and evaporated. The crude residue was purified by silica gel column chromatography (hexanes/EtOAc=9:1v/v) gave TBS protected diastereomeric mixture product (311 mg). The purified product was taken for next step without further analysis. To a stirred solution of TBS protected product (0.702 mmol) in CH_2Cl_2 (4.0 ml), triethylamine (10.6 mmol) and methanesulfonyl chloride (3.44 mmol) were added at $0\text{ }^{\circ}\text{C}$ and the reaction mixture was stirred at the same temperature for 3 h. Excess TEA (10.6 mmol) was added and the reaction mixture was slowly warmed to $45\text{ }^{\circ}\text{C}$ and the temperature was maintained for overnight. Reaction completion was monitored by TLC. Reaction mixture was diluted with CH_2Cl_2 and washed with sat. NaHCO_3 . Organic layer was dried over MgSO_4 , filtered and evaporated. The crude residue was purified by silica gel column chromatography (hexanes/EtOAc=9.8:0.2 v/v) to afforded **10** (214 mg, 16% for three steps) as a white solid: mp $52\text{-}54\text{ }^{\circ}\text{C}$; ^1H NMR (400 MHz, CDCl_3) δ 6.95-6.91 (t, $J = 6.6\text{ Hz}$, 1.2, 1H), 4.51 (s, 1H), 4.43-4.38 (q, $J = 6.6\text{ Hz}$, 1H), 2.34-2.23 (m, 2H), 1.51-1.45 (m, 2H), 1.3 (d, $J = 6.8\text{ Hz}$, 3H), 1.26 (bs, 20H), 0.88 (bm, 12H), 0.13 (d, $J = 6.8\text{ Hz}$, 6H).

(*E*,4*R*,5*S*)-Dihydro-4-hydroxy-5-methyl-3-tetradecylidenefuran-2(3*H*)-one (11). To a solution of **10** (150 mg, 0.35 mmol) in methanol (5 ml), 1M HCl (0.3 ml) was added and the reaction mixture was heated to $60\text{ }^{\circ}\text{C}$ and maintained overnight. The reaction completion was monitored by TLC. Reaction mixture was cooled to room temperature, evaporated in high vacuo. The crude residue dissolved in ethyl acetate, washed with sat. NaHCO_3 solution. Organic layer was dried over MgSO_4 , filtered and evaporated. The crude residue was purified by silica gel column chromatography (hexanes/EtOAc=9:1 v/v) to give **11** (77 mg, 70%) as

off-white solid: mp 48-50 °C; $[\alpha]_{\text{D}}^{20} = 42.6$ ($c=0.1$, CHCl_3); ^1H NMR (400 MHz, CDCl_3) δ 7.0 (t, $J = 8.0$, 1H), 4.55 (d, $J = 6.4$ Hz, 1H), 4.52-4.47 (m, 1H), 2.8-2.2 (m, 2H), 1.92 (bs, 1H), 1.54-1.48 (m, 2H), 1.35 (d, $J = 6.4$ Hz, 3H), 1.3-1.26 (bs, 20H), 0.88 (t, $J = 6.6$ Hz, 3H); ^{13}C NMR (100 MHz, CDCl_3) δ 169.4, 148.6, 129.3, 82.4, 72.2, 31.9, 29.7-29.3, 28.4, 22.6, 19.7, 14.1; IR (neat) 3365, 2919, 2846, 1723, 1681, 1463, 1341, 1265, 1047 cm^{-1} ; HRMS (ESI) m/z calcd for $\text{C}_{19}\text{H}_{34}\text{O}_3$ $[\text{M}+\text{H}]^+$: 311.2586, found: 311.2573; Anal. calculated for $\text{C}_{19}\text{H}_{34}\text{O}_3$: C, 73.50; H, 11.04, found: C, 73.48; H, 11.01.

General procedure for the preparation of compounds 12-21

To a stirred solution of lithium diisopropylamide (4.5 eq., 2.0 M in heptane) in THF at -78 °C, was added a solution of **1** (1eq.) in THF dropwise via syringe under N_2 atmosphere. After 2 h of stirring, a solution of proper aldehyde (1.2eq.) in dry THF and HMPA (1:1, v/v) was added dropwise via syringe at -78 °C and the reaction mass was allowed to warm to -30 °C over a period of 3 h and the same temperature was maintained for 3 h. The reaction mixture was quenched with sat. NH_4Cl and extracted with EtOAc (three times). Combined organic layer washed with brine, dried over MgSO_4 , filtered and evaporated. The crude residue was purified by silica gel column chromatography (EtOAc/ $\text{CH}_2\text{Cl}_2=0-20\%$ EtOAc) gave diastereomeric mixture product. The purified product was taken for next step without further analysis. To a stirred solution of above product (1eq.) in DMF at RT, imidazole (2.0 eq.) and tert-Butyldimethylchlorosilane (1.2 eq.) were added under N_2 atmosphere and the reaction mixture was stirred overnight. Reaction mixture was quenched with sat. NaHCO_3 and extracted with EtOAc. Organic layer was dried over MgSO_4 , filtered and evaporated. The crude residue was purified by silica gel column chromatography (hexanes/EtOAc=9:1v/v) gave TBS protected diastereomeric mixture product. The purified product was taken for next step without further analysis. To a stirred solution of TBS protected product (1 eq.) in CH_2Cl_2 , triethylamine (15 eq.) and methanesulfonyl chloride (5 eq.) were added at 0 °C and the reaction mixture was stirred at the same temperature for 3 h. Excess TEA (15 eq.) was added and the reaction mixture was slowly warmed to 45 °C and the temperature was maintained overnight. Reaction completion was monitored by TLC. Reaction mixture was diluted with CH_2Cl_2 and washed with sat. NaHCO_3 . Organic layer was dried over MgSO_4 , filtered and evaporated. The crude residue was purified by silica gel column chromatography (hexanes/EtOAc=9.8:0.2 v/v).

(*E,4S,5S*)-Dihydro-4-(*tert*-butyldimethylsilyl)-5-methyl-3-butyldenefuran-2(3*H*)-one (12)

Waxy solid, yield 13% (for 3 steps): mp 32-34 °C; ¹H NMR (400 MHz, CDCl₃): δ 6.8 (t, *J* = 7.8 Hz, 1H), 4.8 (d, *J* = 4.8 Hz, 1H), 4.45 (m, 1H), 2.38-2.25 (m, 2H), 1.57-1.48 (m, 2H), 1.37 (d, *J* = 6.4 Hz, 3H), 0.98 (t, *J* = 7.2 Hz, 3H), 0.89 (bs, 9H), 0.11 (s, 6H).

(*E,4S,5S*)-Dihydro-4-(*tert*-butyldimethylsilyl)-5-methyl-3-hexyldenefuran-2(3*H*)-one (13)

Colorless oil, yield 14% (for 3 steps): ¹H NMR (400 MHz, CDCl₃) δ 6.67 (t, *J* = 7.2 Hz, 1H), 4.7 (d, *J* = 4.8 Hz, 1H), 4.35 (m, 1H), 2.28-2.14 (m, 2H), 1.43-1.32 (m, 2H), 1.26 (d, *J* = 6 Hz, 3H), 1.22-1.17 (bm, 4H), 0.78 (bs, 12H), 0.00 (s, 6 H).

(*E,4S,5S*)-Dihydro-4-(*tert*-butyldimethylsilyl)-5-methyl-3-octayldenefuran-2(3*H*)-one (14)

Colorless oil, yield: 14% (for 3 steps): ¹H NMR (400 MHz, CDCl₃) δ 6.8-6.76 (t, *J* = 7.6Hz, 1H), 4.83 (d, *J* = 4.4 Hz, 1H), 4.45-4.4 (m, 1H), 2.37-2.25 (m, 2H), 1.53-1.41 (m, 2H), 1.37 (d, *J* = 6.4 Hz, 3H), 1.32-1.27 (bm, 8H), 0.89 (bs, 9H), 0.88 (t, *J* = 7.6 Hz, 3H), 0.11 (s, 6H).

(*E,4S,5S*)-Dihydro-4-(*tert*-butyldimethylsilyl)-5-methyl-3-nonyldenefuran-2(3*H*)-one (15)

Colorless oil, yield 12% (for 3 steps): ¹H NMR (400 MHz, CDCl₃) δ 6.8-6.76 (t, *J* = 7.8Hz, 1H), 4.84 (d, *J* = 4.8 Hz, 1H), 4.45-4.12 (m, 1H), 2.39-2.25 (m, 2H), 1.53-1.41 (m, 2H), 1.37 (d, *J* = 6.4 Hz, 3H), 1.27 (bs, 10H), 0.89 (bs, 9H), 0.88 (t, *J* = 8 Hz, 3H), 0.11 (s, 6H).

(*E,4S,5S*)-3-Decylidene-dihydro-4-(*tert*-butyldimethylsilyl)-5-methylfuran-2(3*H*)-one (16)

Colorless oil, yield 13% (for 3 steps): ¹H NMR (400 MHz, CDCl₃) δ 6.8-6.76 (dt, *J* = 1.4, 6.8Hz, 1H), 4.84 (d, *J* = 4.8 Hz, 1H), 4.47-4.41 (m, 1H), 2.39-2.25 (m, 2H), 1.53-1.43 (m, 2H), 1.37 (d, *J* = 6.8 Hz, 3H), 1.32-1.26 (bs, 12H), 0.89 (bs, 9H), 0.88 (t, *J* = 7.2 Hz, 3H), 0.11 (s, 6H).

(*E,4S,5S*)-Dihydro-4-(*tert*-butyldimethylsilyl)-5-methyl-3-undecyldenefuran-2(3*H*)-one (17)

Colorless oil, yield 13% (for 3 steps): ¹H NMR (400 MHz, CDCl₃) δ 6.8-6.64 (t, *J* = 7.8Hz, 1H), 4.72 (d, *J* = 4.8 Hz, 1H), 4.35-4.29 (m, 1H), 2.28-2.14 (m, 2H), 1.42-1.31 (m, 2H), 1.26 (d, *J* = 6 Hz, 3H), 1.15 (bs, 14H), 0.78 (bs, 9H), 0.77 (t, *J* = 6.8 Hz, 3H), 0.0 (s, 6H).

(*E,4S,5S*)-3-Dodecylidene-dihydro-4-(*tert*-butyldimethylsilyl)-5-methylfuran-2(3*H*)-one

(18)

Colorless oil, yield 13% (for 3 steps): ^1H NMR (400 MHz, CDCl_3) δ 6.8-6.76 (t, $J = 7.6$ Hz, 1H), 4.84 (d, $J = 4.4$ Hz, 1H), 4.47-4.41 (m, 1H), 2.39-2.25 (m, 2H), 1.53-1.41 (m, 2H), 1.37 (d, $J = 6.4$ Hz, 3H), 1.26 (bs, 16H), 0.89 (bs, 9H), 0.88 (t, $J = 7.6$ Hz, 3H), 0.11 (s, 6H).

(*E,4S,5S*)-Dihydro-4-(*tert*-butyldimethylsilyl)-5-methyl-3-tridecyldenefuran-2(3*H*)-one (19)

Colorless oil, yield 14% (for 3 steps): ^1H NMR (400 MHz, CDCl_3) δ 6.8-6.76 (dt, $J = 1.4, 7.6$ Hz, 1H), 4.83 (d, $J = 4.4$ Hz, 1H), 4.46-4.4 (m, 1H), 2.37-2.25 (m, 2H), 1.53-1.42 (m, 2H), 1.37 (d, $J = 6.4$ Hz, 3H), 1.26 (bs, 18 H), 0.89 (bs, 9H), 0.88 (t, $J = 7.2$ Hz, 3H), 0.11 (s, 6H).

(*E,Z,4S,5S*)-Dihydro-4-(*tert*-butyldimethylsilyl)-5-methyl-3-hexadecyldenefuran-2(3*H*)-one (20)

Colorless oil, yield 13% (for 3 steps): ^1H NMR (400 MHz, CDCl_3) δ 6.8 (t, $J = 7.8$ Hz, 1H), 4.84 (d, $J = 4.4$ Hz, 1H), 4.46 (m, 1H), 2.39-2.25 (m, 2H), 1.53-1.41 (m, 2H), 1.37 (d, $J = 6.8$ Hz, 3H), 1.29 (bs, 24H), 0.89 (bs, 9H), 0.88 (t, $J = 7.2$ Hz, 3H), 0.11 (s, 6H).

(*E,4S,5S*)-Dihydro-4-(*tert*-butyldimethylsilyl)-5-methyl-3-octadecyldenefuran-2(3*H*)-one (21)

Colorless oil, yield 13% (for 3 steps): ^1H NMR (400 MHz, CDCl_3) δ 6.8-6.75 (dt, $J = 1.6, 7.6$ Hz, 1H), 4.83 (d, $J = 4.4$ Hz, 1H), 4.45-4.4 (m, 1H), 2.37-2.27 (m, 2H), 1.51-1.4 (m, 2H), 1.37 (d, $J = 6.8$ Hz, 3H), 1.25 (bs, 28 H), 0.9 (bs, 9H), 0.88 (t, $J = 7.2$ Hz, 3H), 0.11 (s, 6H).

General procedure for the preparation of compounds 22-31

To a stirred solution of above TBS protected product (0.2 mmol) in methanol (4 ml), 1M aq. HCl (0.2 ml) was added, and the reaction mixture was slowly heated to 60 °C and maintained overnight. The reaction completion was monitored by TLC. Reaction mixture was cooled to room temperature, volatiles were evaporated. The crude residue was dissolved in EtOAc, washed with sat. NaHCO_3 . Organic layer was dried over MgSO_4 , filtered and evaporated. The crude residue was purified by silica gel column chromatography (hexanes/EtOAc=4:1 v/v).

(E,4S,5S)-3-Butylidene-dihydro-4-hydroxy-5-methylfuran-2(3H)-one (22). Compound **22** was obtained as waxy white solid (65%): mp 44-46 °C; $[\alpha]_{\text{D}}^{20} = -174.7$ (c=1.2, CHCl₃); ¹H NMR (400 MHz, CDCl₃) δ 6.9 (dt, $J = 6.4, 1.4$ Hz, 1H), 4.8 (t, $J = 5.8$ Hz, 1H), 4.57-4.5 (m, 1H), 2.44-2.33 (m, 2H), 1.9 (d, $J = 7.2$ Hz, 1H) 1.62-1.53 (m, 2H), 1.45 (d, $J = 6.8$ Hz, 3H), 0.98 (t, $J = 7.2$ Hz, 3H); ¹³C NMR (100 MHz, CDCl₃) δ 170.0, 147.5, 130.7, 78.7, 67.7, 31.7, 21.7, 13.9, 13.8; IR (neat): 3415, 2960, 1731, 1674, 1196, 1035, 987 cm⁻¹; HRMS (ESI) m/z calcd for C₉H₁₄O₃ [M+H]⁺: 171.1021, found: 171.1017; Anal. calculated for C₉H₁₄O₃: C, 63.51; H, 8.29, found: C, 63.25; H, 8.41.

(E,4S,5S)-3-Hexylidene-dihydro-4-hydroxy-5-methylfuran-2(3H)-one (23). Compound **23** was obtained as waxy white solid (75%): $[\alpha]_{\text{D}}^{20} = -115.3$ (c=2.4, CHCl₃); ¹H NMR (400 MHz, CDCl₃) δ 6.95 (t, $J = 7.8$, 1H), 4.8 (t, $J = 5.2$ Hz, 1H), 4.57-4.5 (m, 1H), 2.45-2.32 (m, 2H), 2.2 (bs, 1H) 1.55-1.5 (m, 2H), 1.47 (d, $J = 6.8$ Hz, 3H), 1.39-1.29 (m, 4H), 0.91 (t, $J = 6.8$ Hz, 3H); ¹³C NMR (100 MHz, CDCl₃) δ 170.2, 147.8, 130.4, 78.9, 67.7, 31.4, 29.8, 28.1, 22.4, 13.9; IR (neat): 3408, 2928, 1728, 1674, 1200, 1034, 984 cm⁻¹; HRMS (ESI) m/z calcd for C₁₁H₁₈O₃ [M+H]⁺: 199.1334, found: 199.1341; Anal. calculated for C₁₁H₁₈O₃: C, 66.64; H, 9.15, found: C, 66.95; H, 9.17.

(E,4S,5S)-Dihydro-4-hydroxy-5-methyl-3-octylidene-furan-2(3H)-one (24). Compound **24** was obtained as a syrupy solid (66%): mp 42-44 °C; $[\alpha]_{\text{D}}^{25} = -123.1$ (c=0.092, CHCl₃); ¹H NMR (400 MHz, CDCl₃) δ 6.93-6.89 (dt, $J = 0.8, 8.2$ Hz, 1H), 4.87 (bs, 1H), 4.56-4.52 (m, 1H), 2.54 (bs, 1H), 2.44-2.23 (m, 2H), 1.54-1.49 (m, 2H), 1.46 (d, $J = 6.4$ Hz, 3H), 1.35-1.27 (bm, 8H), 0.88 (t, $J = 6.8$ Hz, 3H); ¹³C NMR (100 MHz, CDCl₃) δ 170.4, 147.9, 130.4, 79.1, 67.6, 31.7, 29.8-29, 28.4, 22.6, 14, 13.9; IR (neat) 3391, 2925, 2852, 1722, 1676, 1205, 1037, 982 cm⁻¹; HRMS (ESI) m/z calcd for C₁₃H₂₂O₃ [M+H]⁺: 227.1647, found: 227.1647; Anal. calculated for C₁₃H₂₂O₃: C, 68.99; H, 9.80, found: C, 69.32; H, 9.91.

(E,4S,5S)-Dihydro-4-hydroxy-5-methyl-3-nonylidene-furan-2(3H)-one (25). Compound **25** was obtained as low melting solid (72%): mp 45-47 °C; $[\alpha]_{\text{D}}^{25} = -110.2$ (c=0.104, CHCl₃); ¹H NMR (400 MHz, CDCl₃) δ 6.93-6.89 (dt, $J = 1.2, 8.4$ Hz, 1H), 4.82 (t, $J = 4.8$ Hz, 1H), 4.57-4.5 (m, 1H), 2.45-2.34 (m, 2H), 1.82 (bs, 1H), 1.56-1.48 (m, 2H), 1.47 (d, $J = 6.8$ Hz, 3H), 1.39-1.27 (bm, 10H), 0.88 (t, $J = 6.8$ Hz, 3H); ¹³C NMR (100 MHz, CDCl₃) δ 170, 147.8, 130.4, 78.7, 67.7, 31.8, 29.8-29.1, 28.4, 22.6, 14, 13.9; IR (neat) 3381, 2921, 2844,

1722, 1688, 1456, 1208, 1039, 980 cm^{-1} ; HRMS (ESI) m/z calcd for $\text{C}_{14}\text{H}_{24}\text{O}_3$ $[\text{M}+\text{H}]^+$: 241.1804, found: 241.1804; Anal. calculated for $\text{C}_{14}\text{H}_{24}\text{O}_3$: C, 69.96; H, 10.07, found: C, 69.56; H, 9.95.

(*E*,4*S*,5*S*)-3-Decylidene-dihydro-4-hydroxy-5-methylfuran-2(3*H*)-one, (-)-licunolide B (26). Compound **26** was obtained as off-white solid (77%): mp 51-53 °C; $[\alpha]_{\text{D}}^{25} = -112.9$ ($c=0.096$, CHCl_3): ^1H NMR (400 MHz, CDCl_3) δ 6.94-6.89 (dt, $J = 1.2, 8.4$ Hz, 1H), 4.82 (t, $J = 5.2$ Hz, 1H), 4.56-4.51 (m, 1H), 2.47-2.23 (m, 2H), 2.36 (bs, 1H), 1.53-1.49 (m, 2H), 1.46 (d, $J = 6.8$ Hz, 3H), 1.33-1.26 (m, 12H), 0.88 (t, $J = 7.2$ Hz, 3H); ^{13}C NMR (100 MHz, CDCl_3) δ 170.3, 147.9, 130.4, 79, 67.6, 31.8, 29.8-29.2, 28.4, 22.6, 14.1, 13.9; IR (neat) 3382, 2921, 2848, 1726, 1694, 1457, 1203, 1028, 980 cm^{-1} ; HRMS (ESI) m/z calcd for $\text{C}_{15}\text{H}_{26}\text{O}_3$ $[\text{M}+\text{H}]^+$: 255.196, found: 255.196; Anal. calculated for $\text{C}_{15}\text{H}_{26}\text{O}_3$: C, 70.83; H, 10.30, found: C, 70.56; H, 10.18.

(*E*,4*S*,5*S*)-Dihydro-4-hydroxy-5-methyl-3-undecylidenefuran-2(3*H*)-one (27). Compound **27** was obtained as off-white solid (70%): mp 58-60 °C; $[\alpha]_{\text{D}}^{20} = -111.5$ ($c=0.072$, CHCl_3); ^1H NMR (400 MHz, CDCl_3) δ 6.95-6.91 (dt, $J = 8.0, 1.4$ Hz, 1H), 4.81 (t, $J = 5.4$ Hz, 1H), 4.56-4.5 (m, 1H), 2.43-2.34 (m, 2H), 2.3 (d, $J = 7.2$ Hz, 1H), 1.53-1.48 (m, 2 H), 1.46 (d, $J = 6.8$ Hz, 3H), 1.37-1.26 (bs, 14H), 0.88 (t, $J = 6.8$ Hz, 3H); ^{13}C NMR (100 MHz, CDCl_3) δ 170.1, 147.8, 130.4, 78.8, 67.7, 31.9, 29.3-29.8, 28.4, 22.7, 14.1, 13.9; IR (neat) 3381, 2920, 2846, 1723, 1688, 1457, 1262, 1026, 982 cm^{-1} ; HRMS (ESI) m/z calcd for $\text{C}_{16}\text{H}_{28}\text{O}_3$ $[\text{M}+\text{H}]^+$: 269.2117, found: 269.2118; Anal. calculated for $\text{C}_{16}\text{H}_{28}\text{O}_3$: C, 71.60; H, 10.52, found: C, 71.89; H, 10.63.

(*E*,4*S*,5*S*)-3-Dodecylidene-dihydro-4-hydroxy-5-methylfuran-2(3*H*)-one, (-)-lincomolide B (28). Compound **28** was obtained as off-white solid (68%): mp 63-65 °C; $[\alpha]_{\text{D}}^{25} = -90.2$ ($c=0.084$, CHCl_3): ^1H NMR (400 MHz, CDCl_3) δ 6.93-6.89 (dt, $J = 0.8, 8.2$ Hz, 1H), 4.87 (bs, 1H), 4.56-4.52 (m, 1H), 2.45 (bs, 1H), 2.45-2.36 (m, 2H), 1.53-1.49 (m, 2H), 1.46 (d, $J = 6.8$ Hz, 3H), 1.26 (bs, 16H), 0.88 (t, $J = 6.6$ Hz, 3H); ^{13}C NMR (100 MHz, CDCl_3) δ 170.3, 147.9, 130.4, 79, 67.6, 31.9, 29.8-29.3, 28.4, 22.6, 14.1, 13.9; IR (neat) 3381, 2920, 2847, 1721, 1692, 1460, 1215, 1031, 983 cm^{-1} ; HRMS (ESI) m/z calcd for $\text{C}_{17}\text{H}_{30}\text{O}_3$ $[\text{M}+\text{H}]^+$: 283.2273, found: 283.2273; Anal. calculated for $\text{C}_{17}\text{H}_{30}\text{O}_3$: C, 72.30; H, 10.71, found: C, 72.78; H, 11.84.

(*E*,4*S*,5*S*)-Dihydro-4-hydroxy-5-methyl-3-tridecylidenefuran-2(3*H*)-one (29). Compound **29** was obtained as off-white solid (78%): mp 67-68 °C; $[\alpha]_{\text{D}}^{25} = -109.7$ ($c=0.084$, CHCl_3); ^1H NMR (400 MHz, CDCl_3) δ 6.93-6.89 (dt, $J = 1.2, 8.4$ Hz, 1H), 4.81 (bs, 1H), 4.56-4.5 (m, 1H), 2.45-2.36 (m, 2H), 2.54 (d, $J = 5.6$ Hz, 1H), 1.55-1.48 (m, 2H), 1.46 (d, $J = 6.8$ Hz, 3H), 1.25 (bs, 18H), 0.88 (t, $J = 6.8$ Hz, 3H); ^{13}C NMR (100 MHz, CDCl_3) δ 170.2, 147.8, 130.4, 78.9, 67.7, 31.9, 29.8-29.3, 28.4, 22.6, 14.1, 13.9; IR (neat) 3382, 2917, 2846, 1723, 1691, 1454, 1208, 1033, 987 cm^{-1} ; HRMS (ESI) m/z calcd for $\text{C}_{18}\text{H}_{32}\text{O}_3$ $[\text{M}+\text{H}]^+$: 297.243, found: 297.243; Anal. calculated for $\text{C}_{18}\text{H}_{32}\text{O}_3$: C, 72.93; H, 10.88, found: C, 72.74; H, 10.66.

(*E*,4*S*,5*S*)-3-Hexadecylidene-dihydro-4-hydroxy-5-methylfuran-2(3*H*)-one, (-)-isodihydromahubanolid B (30). Compound **30** was obtained as off-white solid (74%): mp 78-80 °C; $[\alpha]_{\text{D}}^{20} = -79.8$; ^1H NMR (400 MHz, CDCl_3) δ 6.98 (t, $J = 7.8$ Hz, 1H), 4.84 (t, $J = 5.6$ Hz, 1H), 4.56-4.5 (m, 1H), 2.45-2.32 (m, 2H), 1.65 (bs, 1H) 1.54-1.48 (m, 2H), 1.47 (d, $J = 6.8$ Hz, 3H), 1.25 (bs, 24H), 0.89 (t, $J = 6.8$ Hz, 3H); ^{13}C NMR (100 MHz, CDCl_3) δ 169.9, 147.8, 130.4, 78.7, 67.7, 31.9, 29.8-29.3, 28.4, 22.7, 14.1, 13.9; IR (neat): 3880, 2918, 2847, 1724, 1690, 1457, 1265, 1023, 987 cm^{-1} ; HRMS (ESI) m/z calcd for $\text{C}_{21}\text{H}_{38}\text{O}_3$ $[\text{M}+\text{H}]^+$: 339.2899, found: 339.2876; Anal. calculated for $\text{C}_{21}\text{H}_{38}\text{O}_3$: C, 74.51; H, 11.31, found: C, 74.38; H, 11.33.

(*E*,4*S*,5*S*)-Dihydro-4-hydroxy-5-methyl-3-octadecylidenefuran-2(3*H*)-one (31). Compound **31** was obtained as off-white solid (72%): mp 83-85 °C; $[\alpha]_{\text{D}}^{20} = -64.8$ ($c=0.08$, CHCl_3); ^1H NMR (400 MHz, CDCl_3) δ 6.95-6.91 (dt, $J = 8.0, 1.4$ Hz, 1H), 4.81 (t, $J = 5.8$ Hz, 1H), 4.56-4.50 (m, 1H), 2.45-2.34 (m, 2H), 2.0 (d, $J = 6.8$ Hz, 1H), 1.55-1.49 (m, 2H), 1.48 (d, $J = 5.6$ Hz, 3H), 1.3-1.25 (bs, 28H), 0.88 (t, $J = 6.8$ Hz, 3H); ^{13}C NMR (100 MHz, CDCl_3) δ 170.1, 147.8, 130.4, 78.8, 67.7, 31.9, 29.3-29.8, 28.4, 22.7, 14.1, 13.9; IR (neat) 3381, 2913, 2846, 1723, 1689, 1455, 1213, 1026, 987 cm^{-1} ; HRMS (ESI) m/z calcd for $\text{C}_{23}\text{H}_{42}\text{O}_3$ $[\text{M}+\text{H}]^+$: 367.3212, found: 367.3214; Anal. calculated for $\text{C}_{23}\text{H}_{42}\text{O}_3$: C, 75.36; H, 11.55, found: C, 75.09; H, 11.43.

Author Contributions

The manuscript was written through contributions by all authors. All authors approved the final version of manuscript.

Acknowledgement

We declare competing financial interest in the utility of marliolide derivatives. This research was supported by the National Research Foundation of Korea (NRF) grant funded by the Korea Ministry of Science (NRF-2017R1D1A1B03036116), the Bio & Medical Technology Development Program of the National Research Foundation of Korea (NRF) funded by the Ministry of Science, ICT & Future Planning (No. 2012M3A9C1053532), and the GRRC program of Gyeonggi province (GRRC-DONGGUK2016-B04).

Keywords

HO-1, Heme oxygenase-1; NRF2, NF-E2-related factor 2; KEAP1, Kelch-like ECH-associated protein 1; ARE, antioxidant response element; GCLC, glutamate-cysteine ligase modifier catalytic unit; MEF, mouse embryonic fibroblast; DMBA, 12-Dimethylbenz[a]anthracene; TPA, 12-*O*-Tetradecanoylphorbol-13-acetate; 8-OH-G, 8-hydroxyguanosine; 4-HNE, 4-hydroxynonenal.

Appendix A. Supplementary data

Supplementary data related to this article can be found at.

References

- [1] H. Sies, C. Berndt, D.P. Jones, Oxidative Stress, *Annu Rev Biochem*, 86 (2017) 715-748.
- [2] M. Schieber, N.S. Chandel, ROS function in redox signaling and oxidative stress, *Curr Biol*, 24 (2014) R453-462.
- [3] T. Suzuki, M. Yamamoto, Stress-sensing mechanisms and the physiological roles of the Keap1-Nrf2 system during cellular stress, *J Biol Chem*, 292 (2017) 16817-16824.
- [4] N.G. Abraham, J.M. Junge, G.S. Drummond, Translational Significance of Heme Oxygenase in Obesity and Metabolic Syndrome, *Trends Pharmacol Sci*, 37 (2016) 17-36.
- [5] S.W. Ryter, J. Alam, A.M. Choi, Heme oxygenase-1/carbon monoxide: from basic science to therapeutic applications, *Physiol Rev*, 86 (2006) 583-650.
- [6] T. Jansen, M. Hortmann, M. Oelze, B. Opitz, S. Steven, R. Schell, M. Knorr, S. Karbach, S. Schuhmacher, P. Wenzel, T. Munzel, A. Daiber, Conversion of biliverdin to bilirubin by biliverdin reductase contributes to endothelial cell protection by heme oxygenase-1-evidence for direct and indirect antioxidant actions of bilirubin, *J Mol Cell Cardiol*, 49 (2010) 186-195.
- [7] R. Gozzelino, M.P. Soares, Coupling heme and iron metabolism via ferritin H chain, *Antioxid Redox Signal*, 20 (2014) 1754-1769.
- [8] K.D. Poss, S. Tonegawa, Reduced stress defense in heme oxygenase 1-deficient cells, *Proc Natl Acad Sci U S A*, 94 (1997) 10925-10930.
- [9] A. Yachie, Y. Niida, T. Wada, N. Igarashi, H. Kaneda, T. Toma, K. Ohta, Y. Kasahara, S. Koizumi, Oxidative stress causes enhanced endothelial cell injury in human heme oxygenase-1 deficiency, *J Clin Invest*, 103 (1999) 129-135.
- [10] Y. Zhao, Y.-W. Guo, W. Zhang, Rotundifolides A and B, Two New Enol-Derived Butenolactones from the Bark of *Litsea rotundifolia* var. *oblongifolia*, *Helv Chim Acta*, 88 (2005) 349-353.
- [11] B.M. Claros, A.J. da Silva, M.L. Vasconcellos, A.P. de Brito, G.G. Leitao, Chemical constituents of two *Mollinedia* species, *Phytochemistry*, 55 (2000) 859-862.
- [12] R. Motterlini, R. Foresti, Heme oxygenase-1 as a target for drug discovery, *Antioxid Redox Signal*, 20 (2014) 1810-1826.
- [13] M.P. Soares, I. Marguti, A. Cunha, R. Larsen, Immunoregulatory effects of HO-1: how does it work?, *Curr Opin Pharmacol*, 9 (2009) 482-489.
- [14] Y. Naito, T. Takagi, Y. Higashimura, Heme oxygenase-1 and anti-inflammatory M2 macrophages, *Arch Biochem Biophys*, 564 (2014) 83-88.

- [15] M.L. Ferrandiz, I. Devesa, Inducers of heme oxygenase-1, *Curr Pharm Des*, 14 (2008) 473-486.
- [16] Q. Ma, X. He, Molecular basis of electrophilic and oxidative defense: promises and perils of Nrf2, *Pharmacol Rev*, 64 (2012) 1055-1081.
- [17] K. Mailar, W.J. Choi, The first asymmetric synthesis of marliolide from readily accessible carbohydrate as chiral template, *Carbohydr Res*, 432 (2016) 31-35.
- [18] S.I. Lee, J.H. Jang, G.S. Hwang, D.H. Ryu, Asymmetric synthesis of alpha-alkylidene-beta-hydroxy-gamma-butyrolactones via enantioselective tandem Michael-aldol reaction, *J Org Chem*, 78 (2013) 770-775.
- [19] S. Magesh, Y. Chen, L. Hu, Small molecule modulators of Keap1-Nrf2-ARE pathway as potential preventive and therapeutic agents, *Med Res Rev*, 32 (2012) 687-726.
- [20] D.A. Abed, M. Goldstein, H. Albanyan, H. Jin, L. Hu, Discovery of direct inhibitors of Keap1-Nrf2 protein-protein interaction as potential therapeutic and preventive agents, *Acta Pharm Sin B*, 5 (2015) 285-299.
- [21] Y.S. Keum, B.Y. Choi, Molecular and chemical regulation of the Keap1-Nrf2 signaling pathway, *Molecules*, 19 (2014) 10074-10089.
- [22] J.K. Kundu, Y.J. Surh, Inflammation: gearing the journey to cancer, *Mutat Res*, 659 (2008) 15-30.
- [23] L.Y. Chau, Heme oxygenase-1: emerging target of cancer therapy, *J Biomed Sci*, 22 (2015) 22.
- [24] V. Pittala, V. Sorrenti, G. Romeo, A. Acquaviva, C. Di Giacomo, L. Salerno, Therapeutic Potential of Caffeic Acid Phenethyl Ester (CAPE) in Diabetes, *Curr Med Chem*, (2016).
- [25] J.F. Ndisang, Synergistic Interaction Between Heme Oxygenase (HO) and Nuclear-Factor E2- Related Factor-2 (Nrf2) against Oxidative Stress in Cardiovascular Related Diseases, *Curr Pharm Des*, 23 (2017) 1465-1470.
- [26] Y. Cheng, J. Rong, Therapeutic Potential of Heme Oxygenase-1/carbon Monoxide System Against Ischemia-Reperfusion Injury, *Curr Pharm Des*, 23 (2017) 3884-3898.
- [27] Y.L. Xie, J.G. Chu, X.M. Jian, J.Z. Dong, L.P. Wang, G.X. Li, N.B. Yang, Curcumin attenuates lipopolysaccharide/d-galactosamine-induced acute liver injury by activating Nrf2 nuclear translocation and inhibiting NF-kB activation, *Biomed Pharmacother*, 91 (2017) 70-77.
- [28] V. Pittala, L. Vanella, L. Salerno, C. Di Giacomo, R. Acquaviva, M. Raffaele, G. Romeo,

M.N. Modica, O. Prezzavento, V. Sorrenti, Novel Caffeic Acid Phenethyl Ester (Cape) Analogues as Inducers of Heme Oxygenase-1, *Curr Pharm Des*, 23 (2017) 2657-2664.

[29] R.J. Fox, D.H. Miller, J.T. Phillips, M. Hutchinson, E. Havrdova, M. Kita, M. Yang, K. Raghupathi, M. Novas, M.T. Sweetser, V. Vigiotta, K.T. Dawson, C.S. Investigators, Placebo-controlled phase 3 study of oral BG-12 or glatiramer in multiple sclerosis, *The New England journal of medicine*, 367 (2012) 1087-1097.

[30] W. Li, A.N. Kong, Molecular mechanisms of Nrf2-mediated antioxidant response, *Mol Carcinog*, 48 (2009) 91-104.

[31] E. Kansanen, S.M. Kuosmanen, H. Leinonen, A.L. Levonen, The Keap1-Nrf2 pathway: Mechanisms of activation and dysregulation in cancer, *Redox Biol*, 1 (2013) 45-49.

[32] H. Tanaka, Y. Takaya, J. Toyoda, T. Yasuda, M. Sato, J. Murata, H. Murata, K. Kaburagi, O. Iida, K. Sugimura, E. Sakai, Two new butanolides from the roots of *litsea acuminata*, *Phytochemistry Letters*, 11 (2015) 32-36.

[33] I.L. Tsai, C.H. Hung, C.Y. Duh, J.H. Chen, W.Y. Lin, I.S. Chen, Cytotoxic butanolides from the stem bark of Formosan *Lindera communis*, *Planta Med*, 67 (2001) 865-867.

[34] V. Martinez, M. Yoshida, O. Gottlieb, ω -ethyl, ω -ethenyl and ω -ethynyl- α -lactones from *Clinostemon mahuba.*, *Phytochemistry*, 20 (1981) 459-464.

Figure Legends

Fig. 1. Marliolide does not affect the overall integrity of HaCaT cells. (A) Chemical structure of marliolide. (B) Marliolide induces HO-1 in HaCaT cells. HaCaT cells were exposed to marliolide at different concentrations for 24 h (Upper Panel) or at different times (Lower Panel). Western blot was conducted using HO-1 antibody. (C) Marliolide does not induce cell-cycle arrest in HaCaT cells. Marliolide or etoposide was exposed to HaCaT cells for 24 h. The percentage of G1/S arrest was monitored by FACS analysis. Note that etoposide was included as a positive control to induce cell-cycle arrest and subsequent apoptotic cell death. (D) Marliolide is not cytotoxic in HaCaT cells. Marliolide or etoposide was exposed to HaCaT cells and gross cell morphology was observed by phase-contrast microscopy. (E) Marliolide does not induce apoptosis in HaCaT cells. Marliolide or etoposide was exposed to HaCaT cells for various times. Western blot was conducted using cleaved Caspase-3 and cleaved PARP antibodies.

Fig. 2. Induction of HO-1 by marliolide occurs via ARE activation in HaCaT Cells. (A) Generation of HaCaT-ARE-GFP-luciferase cells by lentiviral transduction. (B) Confirmation of ARE luciferase activation in HaCaT-ARE-GFP-luciferase cells by ARE inducer, sulforaphane. HaCaT-ARE-GFP-luciferase cells were exposed to sulforaphane for 24 h and the luciferase activity was measured. (C) Marliolide causes ARE-dependent GFP expression in HaCaT-ARE-GFP-luciferase cells. HaCaT-ARE-GFP-luciferase cells were exposed to marliolide for 24 h and GFP was monitored by fluorescent microscopy. (D) Marliolide induces ARE-dependent luciferase activity in HaCaT-ARE-GFP-luciferase cells in dose- and time-dependent manner. HaCaT-ARE-GFP-luciferase cells were exposed to marliolide at different concentrations (Left Panel) or to marliolide at different times (Right Panel) and the luciferase activity was measured.

Fig. 3. Marliolide induction of HO-1 is mediated by NRF2. (A) The induction of NRF2 by marliolide. HaCaT cells were exposed to marliolide at different concentrations (Upper Panel) or at different times (Lower Panel). Western blot was conducted using NRF2 antibody. (B) Nuclear translocation of NRF2 by marliolide. Marliolide was exposed to HaCaT cells for 6 h and 12 h. The immunofluorescence assay was conducted using NRF2 antibody. (C) The induction of HO-1 by marliolide is dependent on Nrf2 genotype. After genomic DNA was

prepared from Nrf2 (+/+) and Nrf2 (-/-) mouse embryonic fibroblasts (MEFs), the mouse genotyping was conducted. PCR products with 262 and 400 base-pairs (bps) indicate the existence of wild-type and knock-out Nrf2 genotypes, respectively (Upper Panel). After exposure of marliolide to Nrf2 (+/+) and Nrf2 (-/-) MEFs at various times, Western blot analysis was conducted using HO-1 antibody (Lower Panel). (D) Transcriptional activation of HO-1 by marliolide is dependent on NRF2. Total RNA from Nrf2 (+/+) and Nrf2 (-/-) MEFs was prepared and real-time RT-PCR assay was performed using HO-1 specific PCR primers.

Fig. 4. Syntheses of marliolide and its derivatives.

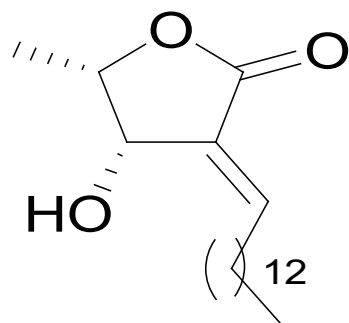
Fig. 5. Structure-activity relationship reveals Michael reaction as a potential mechanism for the induction of NRF2/ARE by marliolide. (A) Marliolide directly binds to KEAP1. HaCaT cell lysates were incubated with biotin or biotinylated marliolide. After immunoprecipitation with streptavidin-agarose bead, Western blot analysis was performed with KEAP1 and NRF2 antibodies. (B) A hypothetical mechanism showing how marliolide directly binds to KEAP1. (C) Effects of marliolide and its derivatives on the induction of HO-1 in HaCaT cells. Marliolide (**2**) and its derivatives (**3-31**) were exposed to HaCaT cells at the concentration of 10 μ M for 6, 12, and 24 h. Western blot was then conducted using HO-1 antibody. (D) Real-time RT-PCR comparing the effects of **2**, **26**, **27**, **28** and **29** on the HO-1 mRNA level in HaCaT cells. After HaCaT cells were exposed to marliolide (**2**) and its derivatives (**26**, **27**, **28** and **29**) at the concentration of 10 μ M for 4 h, 8 h, and 12 h, the real-time RT-PCR was conducted using total RNA. (E) Marliolide derivatives do not affect the viability of HaCaT cells. Marliolide (10 μ M) and its derivatives (10 μ M) were exposed to HaCaT cells for 24 h and the cell viability was measured using MTT assay.

Fig. 6. Marliolide induces NRF2-dependent phase II cytoprotective enzymes and exhibits chemopreventive activity *in vivo*. (A) Topical application of marliolide (10 μ mole) and **29** (10 μ mole) in the back of hairless mice induces NRF2, HO-1 and glutamate-cysteine ligase modifier catalytic unit (GCLC). (B) Marliolide (10 μ mole) exerts inhibitory effects on the number (Upper Panel) and incidence (Lower Panel) of DMBA/TPA-induced papilloma formation in hairless mice. (C) Hematoxylin/Eosin (H/E) staining illustrates that marliolide suppresses the growth of papilloma in the skin of hairless mice induced by DMBA/TPA. (D) Marliolide suppresses the generation of 8-hydroxyguanosine (8-OH-G, Left Panel) and 4-

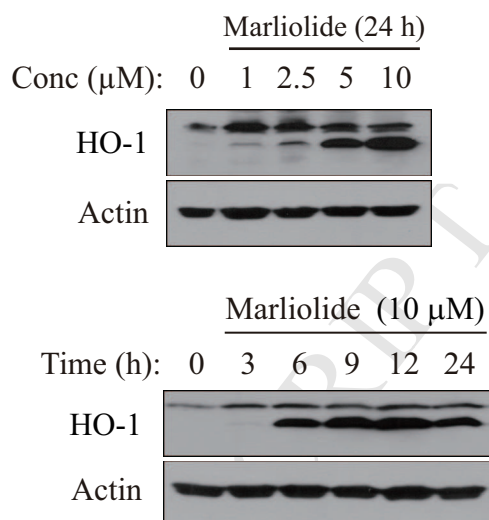
hydroxynonenal (4-HNE, Right Panel) in the skin of hairless mice induced by DMBA/TPA.

ACCEPTED MANUSCRIPT

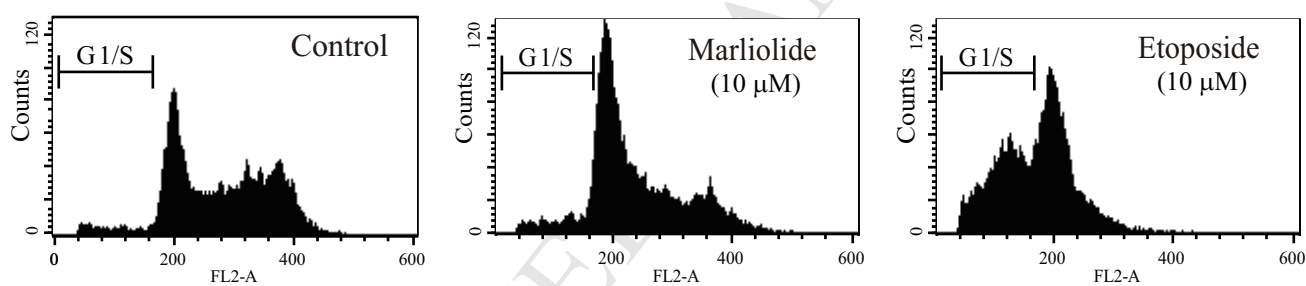
A.



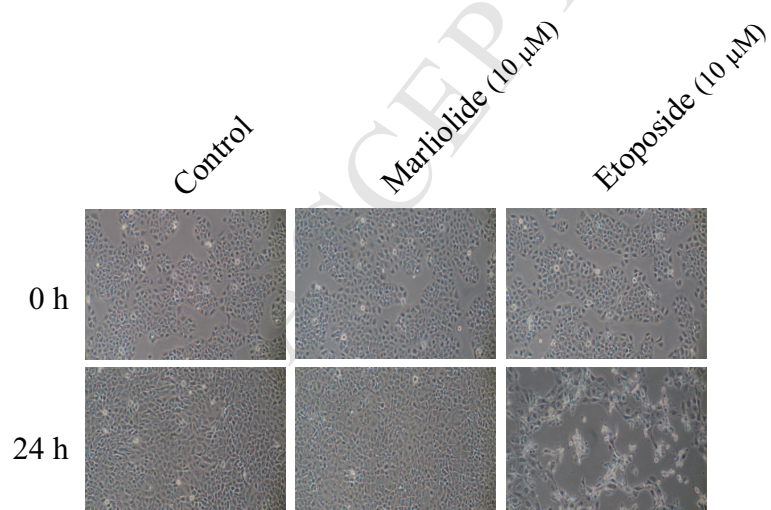
B.



C.



D.



E.

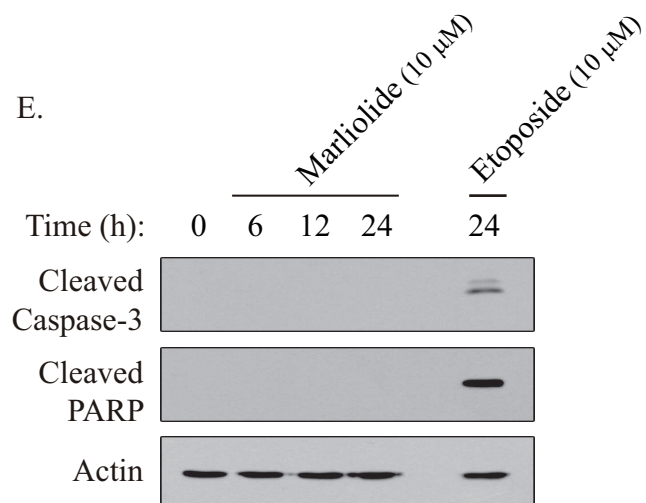


Fig. 1.

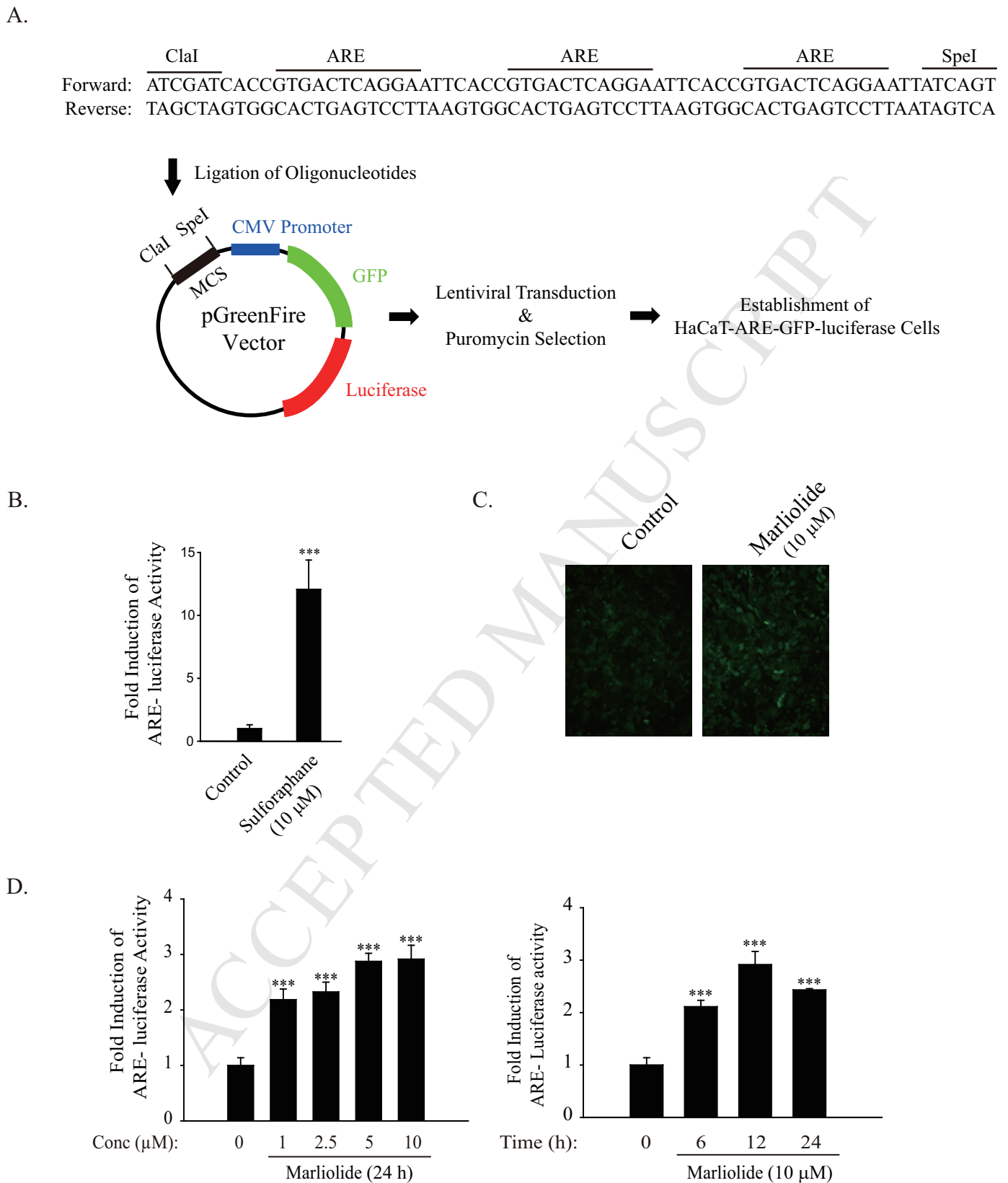


Fig. 2.

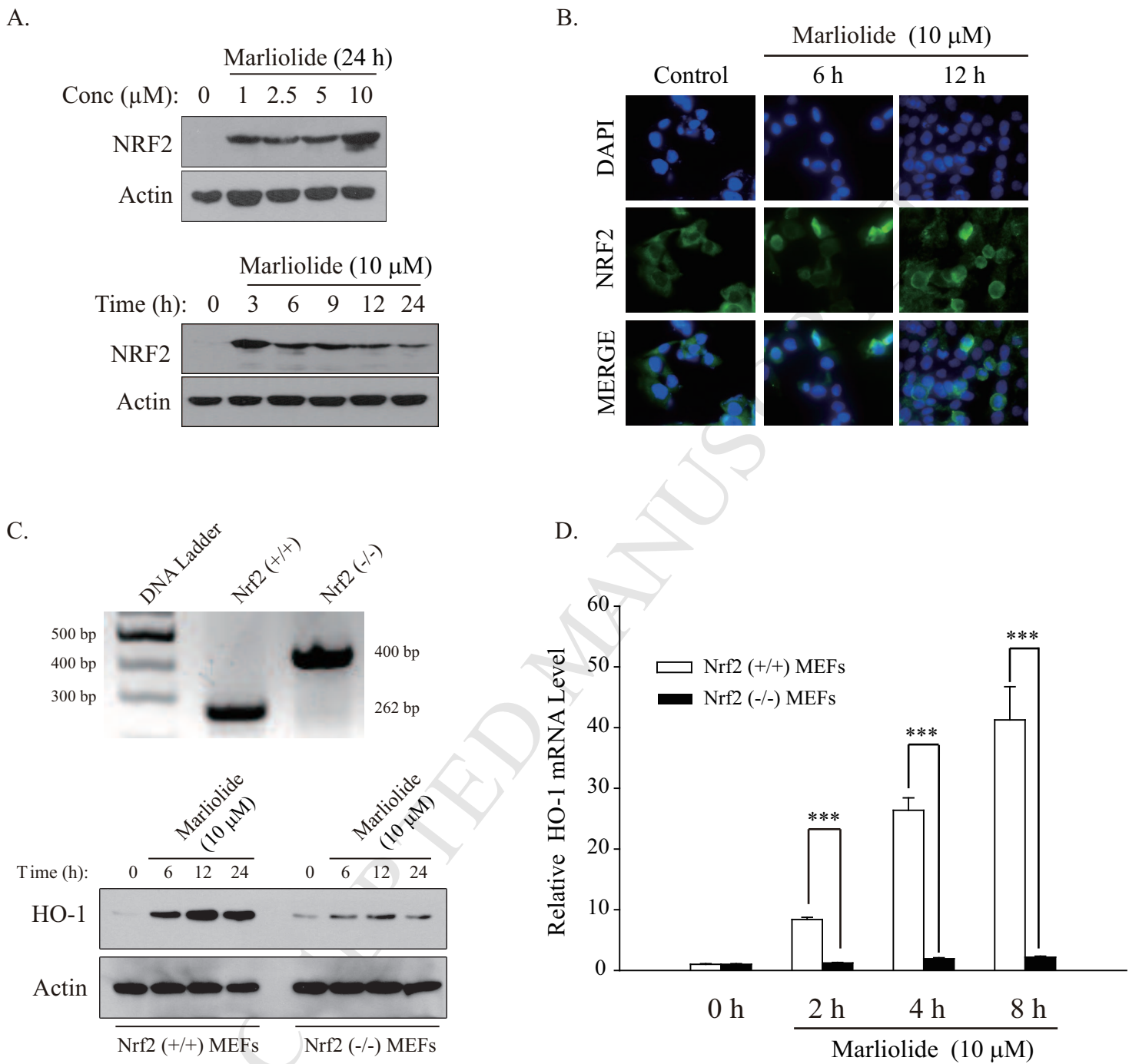
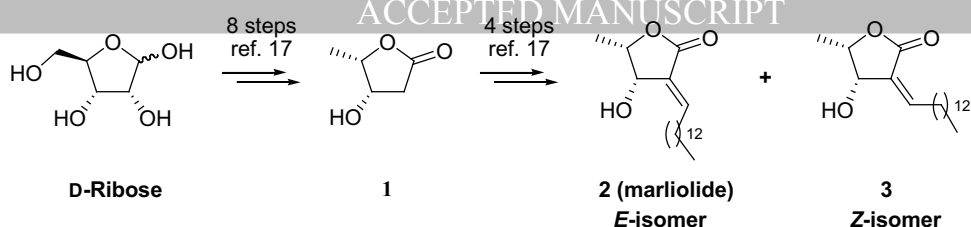
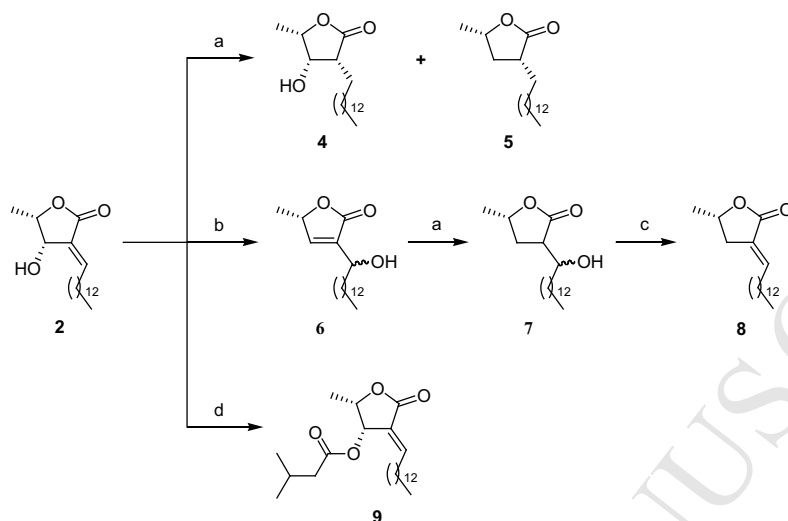


Fig. 3.

A. Synthesis of marliolide and its isomer

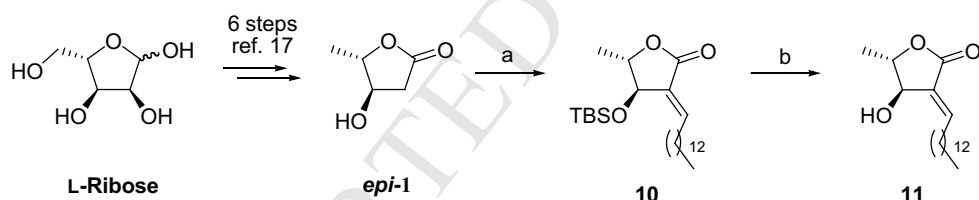


B. Synthesis of marliolide derivatives



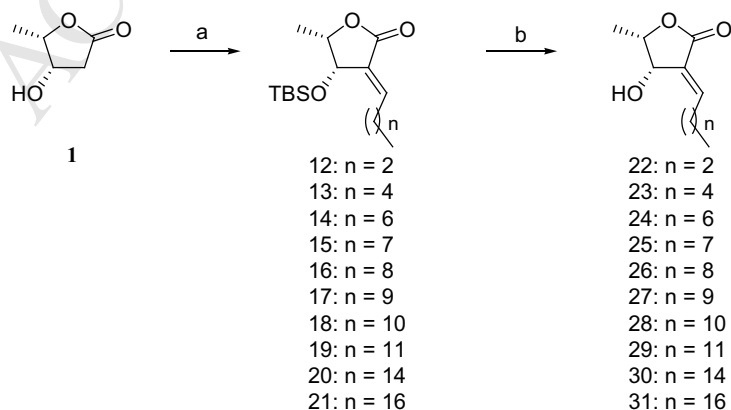
Reagent and conditions: a) Pd/C (5%), H₂, AcOH, EtOH, rt, overnight; b) Jones reagent, acetone, 0 °C to rt, 3 h; c) MsCl, Et₃N, CH₂Cl₂, 0 °C, 3 h, and then Et₃N, 45 °C, overnight; d) Isovaleryl chloride, DMAP, rt, overnight.

C. Synthesis of marliolide epimer



Reagent and conditions: a) i) LDA, myristyl aldehyde, THF, HMPA, -78 °C to -30 °C, 7 h; ii) TBSCl, imidazole, DMF, rt, overnight; iii) MsCl, Et₃N, CH₂Cl₂, 0 °C, 3 h, and then Et₃N, 45 °C, overnight; (b) 1M HCl, MeOH, 60 °C, overnight.

D. Synthesis of marliolide derivatives with different chain length at α-position



Reagent and conditions: a) i) LDA, aldehyde, THF, HMPA, -78 °C to -30 °C, 7 h; ii) TBSCl, imidazole, DMF, rt, overnight; iii) MsCl, Et₃N, CH₂Cl₂, 0 °C, 3 h, and then Et₃N, 45 °C, overnight; (b) 1M HCl, MeOH, 60 °C, overnight.

Fig. 4.

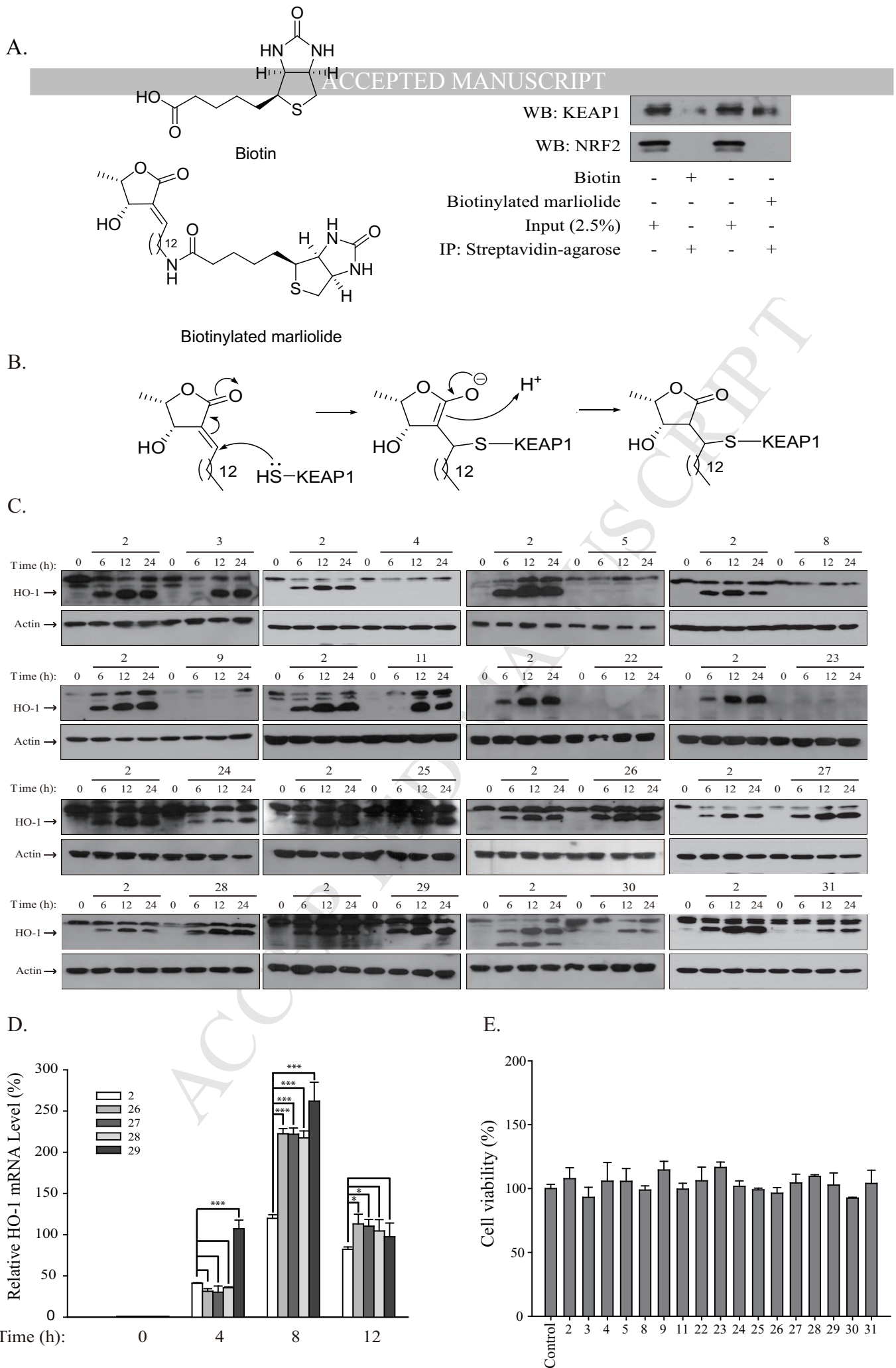


Fig. 5.

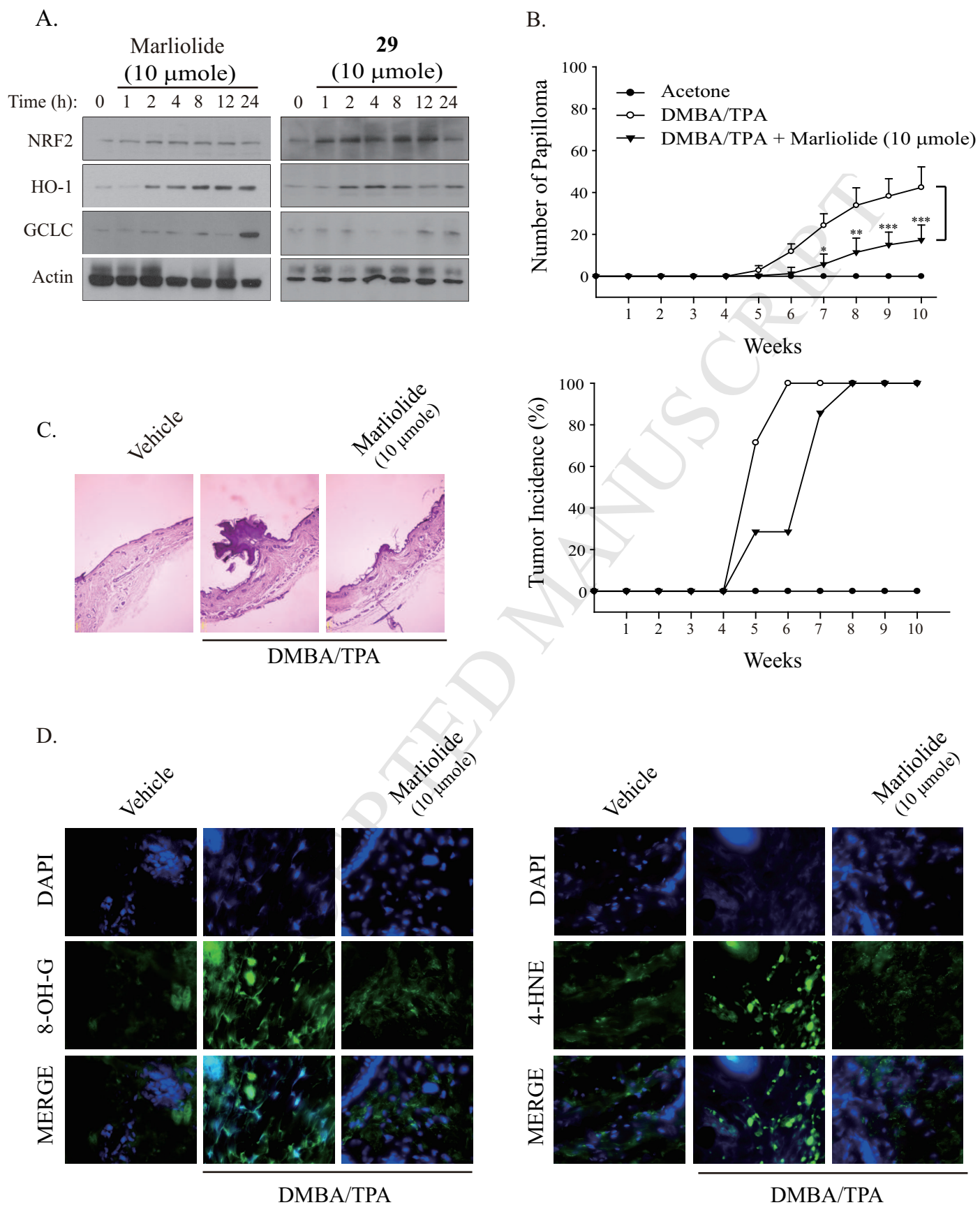


Fig. 6.

Highlights

1. We have identified marliolide as a novel inducer of HO-1.
2. We have identified that the induction of HO-1 by marliolide occurs through activation of NRF2/ARE.
3. We have identified that marliolide activates NRF2/ARE/HO-1 axis by directly binding to KEAP1 via Michael reaction.
4. We have identified that marliolide inhibits DMBA/TPA-induced papilloma formation possibly by suppressing the oxidative damages *in vivo*.